ESAIM: M2AN 48 (2014) 1199–1226
DOI: 10.1051/m2an/2014013

ESAIM: Mathematical Modelling and Numerical Analysis
www.esaim-m2an.org

AN EFFICIENT COMPUTATIONAL FRAMEWORK FOR REDUCED BASIS APPROXIMATION AND *A POSTERIORI* ERROR ESTIMATION OF PARAMETRIZED NAVIER–STOKES FLOWS

Andrea Manzoni[1]

Abstract. We present the current Reduced Basis framework for the efficient numerical approximation of parametrized steady Navier–Stokes equations. We have extended the existing setting developed in the last decade (see *e.g.* [S. Deparis, *SIAM J. Numer. Anal.* **46** (2008) 2039–2067; A. Quarteroni and G. Rozza, *Numer. Methods Partial Differ. Equ.* **23** (2007) 923–948; K. Veroy and A.T. Patera, *Int. J. Numer. Methods Fluids* **47** (2005) 773–788]) to more general affine and nonaffine parametrizations (such as volume-based techniques), to a simultaneous velocity-pressure error estimates and to a fully decoupled Offline/Online procedure in order to speedup the solution of the reduced-order problem. This is particularly suitable for real-time and many-query contexts, which are both part of our final goal. Furthermore, we present an efficient numerical implementation for treating nonlinear advection terms in a convenient way. A residual-based *a posteriori* error estimation with respect to a truth, full-order Finite Element approximation is provided for joint pressure/velocity errors, according to the Brezzi–Rappaz–Raviart stability theory. To do this, we take advantage of an extension of the Successive Constraint Method for the estimation of stability factors and of a suitable fixed-point algorithm for the approximation of Sobolev embedding constants. Finally, we present some numerical test cases, in order to show both the approximation properties and the computational efficiency of the derived framework.

Mathematics Subject Classification. 65M15, 65M60, 65N12, 76D07, 78M34.

Received July 23, 2013. Revised February 5, 2014.
Published online July 15, 2014.

1. Introduction

In this paper we describe some new contributions to the Reduced Basis (RB) approximation and *a posteriori* error estimation of parametrized steady incompressible Navier–Stokes equations. We consider a mixed velocity/pressure formulation of the problem, by addressing the case of (both affine and nonaffine) physical and geometrical parametrizations, and including for the first time the case of external flows around nonaffinely parametrized profiles. Our last goal is to solve real-time numerical simulations and optimization or many-query problems in a very efficient way. Although very strong efforts have been carried out in the last decade to achieve this goal, classical, full-order approximation techniques – such as the Finite Element (FE) method – still entail strong computational costs, so that a further enhancement of the computational efficiency is needed.

Keywords and phrases. Reduced Basis Method, parametrized Navier–Stokes equations, steady incompressible fluids, *a posteriori* error estimation, approximation stability.

[1] SISSA Mathlab – International School for Advanced Studies, Via Bonomea 265, 34136 Trieste, Italy. amanzoni@sissa.it

Article published by EDP Sciences

This is the main reason why *Reduced-Order Models* (ROMs), such as the RB method, have gained increasing popularity in recent years. The goal of a RB method is to approximate the manifold of solutions – *i.e.*, the set of solutions obtained by varying the parameter vector – through a Galerkin projection onto a space spanned by few precomputed snapshots (that is, solutions of the full-order problem at some selected parameters values).

In this work we restrict ourselves to the case of parametrized steady incompressible Navier–Stokes equations. In fact, this problem arises in several fluid flows applications; its rapid and reliable solution represents a remarkable challenge for a ROM, because of nonlinearities, stability and efficiency issues [16].

First of all, the nonlinear nature of Navier–Stokes equations yields serious concerns from both a physical and a computational standpoint. For instance, flow can undergo strong changes (bifurcation phenomena) when the Reynolds number reaches critical values, or even loss of symmetry. Thus, in order to obtain a reliable RB approximation, we require that the manifold of the solutions is smooth and low-dimensional, and that it consists of a branch of nonsingular solutions[2] – the latter is a standard assumption also in the FE method [4,5].

Moreover, we need to face the stability issue related to the calculation of pressure fields. As already in the Stokes case, we can recover the pressure stability at the reduced order level by enriching the reduced velocity space with the so-called *supremizer solutions*. In this way, we manage to fulfill a Brezzi inf-sup condition for the reduced spaces as well. Concerning instead the stability of the approximation, we rely on the *Brezzi–Rappaz–Raviart* (BRR) theory [4,5] for the approximation of branches of nonsingular solutions. We remind that stability factors affect not only the continuous dependence of the solution on data [32], but also the *a posteriori* error estimation ensuring the reliability of the RB method.

Furthermore, for the sake of computational efficiency, we need to properly extend the usual Offline/Online splitting [24, 27] also to nonlinear terms, in order to make both the reduced-order approximation and the error estimation independent of the full-order approximation, and thus very cheap.

In this paper we show how to deal with these issues. For the first time, we address the multifaceted components behind the analysis of the complete steady framework. This includes nonaffine geometrical parametrizations, error bound estimations for velocity/pressure fields jointly, an improved algorithm for the estimation of parametrized lower bounds of stability factors and a modified fixed-point algorithm for the estimation of Sobolev embedding constants, together with rigorous mathematical proofs. In particular, this framework takes advantage of a full uncoupling between the estimation of stability factors and the construction of a reduced space through a greedy selection of velocity-pressure snapshots. This option has been made possible thanks to a recent extension of the *natural-norm* Successive Constraint Method (SCM) [13, 29] to the case of nonlinear parametrized operators, addressed in [18].

More in detail, we present a general parametrized formulation of Navier–Stokes equations (Sect. 2), capable of managing with both (physical and geometrical) affine and nonaffine parametrizations, by relying in the latter case on the Empirical Interpolation Method (EIM) [1]. We also recall the main assumptions required to ensure the well-posedness of both the parametrized formulation and the full-order approximation (Sects. 3–4), pointing out which features must be enforced at the reduced-order level (Sect. 5). Another original contribution of this paper is the setting of *a posteriori* error estimation for velocity and pressure fields jointly (Sect. 6), obtained by exploiting the BRR theory. Moreover, we sketch the main points of the extended SCM [18] for computing lower bounds of stability factors (Sect. 7), and provide a detailed proof of a fixed-point approximation of the Sobolev embedding constants entering in the expression of the error bound (Sect. 8). Finally, we show some numerical tests dealing with low and moderate Reynolds flows in parametrized geometries (Sect. 9). Technical proofs of the stated results are detailed in Appendix A.

We refer to [10, 28] for former contributions on the RB approximation of Stokes problems, and to the recent work [26], for both a stability and *a posteriori* error analysis based on the Brezzi's and the Babuška's inf-sup theories, respectively. In the Navier–Stokes case, after the pioneering works by Peterson [22], Ito and Ravindran [14], a general framework for both RB approximation and *a posteriori* error estimation has been established by Patera,

[2]RB methods might provide reliable approximations also when bifurcation points are included in the parameter space, if the latter is properly sampled; see *e.g.* [12]. Further investigation is ongoing on this issue.

Veroy [31] and Nguyen [21]. This has been further developed in more recent years [7, 8] by considering a complete *natural norm* framework, whereas a first case of simple nonaffine geometrical parametrizations can be found in [23].

2. Parametrized formulation of steady Navier–Stokes equations

The Navier–Stokes (NS) equations provide a model for the flow motion of a viscous Newtonian incompressible fluid. In the steady case, on a spatial domain $\tilde{\Omega} \subset \mathbb{R}^d$, $d = 2, 3$ (which we assume to be piecewise C^2 with convex corners), they read as follows:

$$\begin{cases} -\nu \Delta \mathbf{v} + \delta(\mathbf{v} \cdot \nabla)\mathbf{v} + \nabla p = \mathbf{f} & \text{in } \tilde{\Omega} \\ \nabla \cdot \mathbf{v} = 0 & \text{in } \tilde{\Omega} \\ \mathbf{v} = \mathbf{0} & \text{on } \Gamma_{D_0} \\ \mathbf{v} = \mathbf{g}_D & \text{on } \Gamma_{D_g} \\ -p\mathbf{n} + \nu \dfrac{\partial \mathbf{v}}{\partial \mathbf{n}} = \mathbf{g}_N & \text{on } \Gamma_N, \end{cases} \tag{2.1}$$

where $(\mathbf{v}, p) = (\mathbf{v}(\boldsymbol{\mu}), p(\boldsymbol{\mu}))$ are the velocity and the pressure fields defined on $\tilde{\Omega}$, for some given $\mathbf{f} \in (L^2(\tilde{\Omega}))^d$, $\mathbf{g}_D \in (H^{1/2}(\Gamma_D))^d$, $\mathbf{g}_N \in (H^{1/2}(\Gamma_N))^d$. We denote by $\Gamma_D = \Gamma_{D_0} \cup \Gamma_{D_g}$ the Dirichlet portion of $\partial\tilde{\Omega}$, and by $\mathbf{n}$ the normal unit vector to $\partial\tilde{\Omega}$. We also define the Reynolds number as $\mathrm{Re} = L|\bar{\mathbf{v}}|/\nu$, where L is a characteristic length of the domain, $\bar{\mathbf{v}}$ a typical velocity of the flow and ν the kinematic viscosity. We concentrate on laminar flows, with $Re \in [1, 10^3]$, in the case $d = 2$, although the whole framework keeps holding for the case $d = 3$ as well. Here $\boldsymbol{\mu} = (\boldsymbol{\mu}_p, \boldsymbol{\mu}_g)^T \in \mathcal{D} \subset \mathbb{R}^P$ is a vector of parameters which may characterize either the geometrical configuration – so that $\tilde{\Omega} = \tilde{\Omega}(\boldsymbol{\mu}_g)$ – or physical properties, such as $\nu = \nu(\boldsymbol{\mu}_p)$, boundary data $\mathbf{g}_D = \mathbf{g}_D(\boldsymbol{\mu}_p)$, $\mathbf{g}_N = \mathbf{g}_N(\boldsymbol{\mu}_p)$ or source terms $\mathbf{f} = \mathbf{f}(\boldsymbol{\mu}_p)$. For the sake of notation, we shall distinguish between n_p physical parameters $\boldsymbol{\mu}_p \in \mathcal{D}_p \subset \mathbb{R}^{n_p}$ and $n_g = P - n_p$ physical parameters $\boldsymbol{\mu}_g \in \mathcal{D}_g \subset \mathbb{R}^{n_g}$. Hereon, we omit the dependence on $\boldsymbol{\mu}$ wherever understood, and we adopt the convention that repeated indices are implicitly summed over.

If parameters affect the geometrical configuration (*i.e.* $n_g \geq 1$), we assume that the parameterized configuration $\tilde{\Omega}(\boldsymbol{\mu}_g)$ can be obtained as the image of a reference domain Ω through a parametrized map $T(\cdot; \boldsymbol{\mu}_g) : \mathbb{R}^2 \times \mathcal{D} \to \mathbb{R}^2$. In general, we can deal with original domains made up of K_{dom} mutually nonoverlapping open subdomains $\{\Omega^k\}_{k=1}^{K_{\mathrm{dom}}}$, so that original and reference subdomains can be linked via either an affine or a nonaffine map $T^k(\cdot; \boldsymbol{\mu}_g) : \mathbb{R}^2 \times \mathcal{D} \to \mathbb{R}^2$, *i.e.* $\tilde{\Omega}^k(\boldsymbol{\mu}) = T^k(\Omega^k; \boldsymbol{\mu}_g)$, $1 \leq k \leq K_{\mathrm{dom}}$. See *e.g.* [27] for the regularity assumptions required to the maps $T^k(\cdot; \boldsymbol{\mu}_g)$ in order to ensure the well-posedness of (2.2).

The *parametrized variational formulation* of (2.1) can be obtained by standard integration by parts. When dealing with parametrized geometries, we trace the usual variational formulation, written on $\tilde{\Omega}(\boldsymbol{\mu}_g)$, back on the reference domain Ω, so that: given $\boldsymbol{\mu} \in \mathcal{D} \subset \mathbb{R}^P$, we seek for $(\mathbf{v}, p) = (\mathbf{v}(\boldsymbol{\mu}), p(\boldsymbol{\mu})) \in V \times Q$ such that

$$\begin{cases} \tilde{a}(\mathbf{v}, \mathbf{w}; \boldsymbol{\mu}) + b(p, \mathbf{w}; \boldsymbol{\mu}) + c(\mathbf{v}, \mathbf{v}, \mathbf{w}; \boldsymbol{\mu}) = F(\mathbf{w}; \boldsymbol{\mu}) & \forall \mathbf{w} \in V \\ b(q, \mathbf{v}; \boldsymbol{\mu}) = G(q; \boldsymbol{\mu}) & \forall q \in Q. \end{cases} \tag{2.2}$$

The parametrized forms appearing in (2.2) are defined as follows [23, 28]:

$$a(\mathbf{v}, \mathbf{w}; \boldsymbol{\mu}) = \sum_{k=1}^{K_{\mathrm{dom}}} \int_{\Omega^k} \frac{\partial \mathbf{v}}{\partial x_i} \kappa_{ij}^k(\cdot; \boldsymbol{\mu}) \frac{\partial \mathbf{w}}{\partial x_j}, \qquad b(q, \mathbf{w}; \boldsymbol{\mu}) = -\sum_{k=1}^{K_{\mathrm{dom}}} \int_{\Omega^k} q \chi_{ij}^k(\cdot; \boldsymbol{\mu}) \frac{\partial w_j}{\partial x_i}, \tag{2.3}$$

$$c(\mathbf{v}, \mathbf{w}, \mathbf{z}; \boldsymbol{\mu}) = \sum_{k=1}^{K_{\mathrm{dom}}} \int_{\Omega^k} v_i \, \chi_{ji}^k(\cdot; \boldsymbol{\mu}) \, \frac{\partial w_m}{\partial x_j} z_m, \tag{2.4}$$

whereas the transformation tensors appearing in (2.3)-(2.4) are given by:

$$\boldsymbol{\kappa}^k(\mathbf{x};\boldsymbol{\mu}) = \nu(\boldsymbol{\mu}_p)\left(J_T^k\left(\cdot;\boldsymbol{\mu}_g\right)\right)^{-T}\left(J_T^k\left(\mathbf{x};\boldsymbol{\mu}_g\right)\right)^{-1}|J_T^k\left(\mathbf{x};\boldsymbol{\mu}_g\right)|, \quad 1\le k\le K_{\text{dom}} \tag{2.5}$$

$$\boldsymbol{\chi}^k\left(\mathbf{x};\boldsymbol{\mu}\right) = \left(J_T^k\left(\mathbf{x};\boldsymbol{\mu}_g\right)\right)^{-T}|J_T^k(\mathbf{x};\boldsymbol{\mu}_g)|, \quad 1\le k\le K_{\text{dom}}; \tag{2.6}$$

here $J_T^k:\mathbb{R}^2\times\mathcal{D}_g\to\mathbb{R}^{2\times 2}$ is the Jacobian matrix of the map $T^k(\cdot;\boldsymbol{\mu}_g)$, and $|J_T^k|$ denotes its determinant.

Instead, the linear form is given by

$$F_s(\mathbf{w};\boldsymbol{\mu}) = \sum_{k=1}^{K_{\text{dom}}}\int_{\Omega^k}\mathbf{f}(\boldsymbol{\mu}_p)\cdot\mathbf{w}\;|J_T^k(\cdot;\boldsymbol{\mu}_g)|\mathrm{d}\Omega + \sum_{k=1}^{\bar{K}_{\text{dom}}}\int_{\Gamma_N^k}\mathbf{g}^N(\boldsymbol{\mu}_p)\cdot\mathbf{w}|J_T^k(\cdot;\boldsymbol{\mu}_g)\mathbf{t}|\mathrm{d}\Gamma,$$

where $\mathbf{f}(\boldsymbol{\mu}_p)\in(L^2(\Omega))^2$ is a forcing term per unit mass, $\mathbf{t}$ is the tangential unit vector to the boundary, $\Gamma_N^k=\partial\Omega^k\cap\Gamma_N$ and $\bar{K}_{\text{dom}}\le K_{\text{dom}}$ is the number of subdomains sharing at least one Neumann side. From now on, we assume that $\mathbf{g}^N=\mathbf{0}$. Moreover, we consider a lifting approach to deal with essential (Dirichlet) boundary conditions. Thus, we introduce a lift function $\mathbf{v}_D\in(H^1(\Omega))^2$ such that $\mathbf{v}_D|_{\Gamma_{D_g}}=\mathbf{g}_D$ and $\mathbf{v}_D|_{\Gamma_{D_0}}=\mathbf{0}$, to extend non-homogeneous boundary conditions to the interior of the domain, and denote by

$$\tilde{a}(\mathbf{v}(\boldsymbol{\mu}),\mathbf{w};\boldsymbol{\mu}) = a(\mathbf{v}(\boldsymbol{\mu}),\mathbf{w};\boldsymbol{\mu}) + \mathrm{d}(\mathbf{v}(\boldsymbol{\mu}),\mathbf{w};\boldsymbol{\mu}), \qquad F(\mathbf{w};\boldsymbol{\mu}) = F_s(\mathbf{w};\boldsymbol{\mu}) + F_d(\mathbf{w};\boldsymbol{\mu}),$$

where

$$\mathrm{d}(\mathbf{v},\mathbf{w};\boldsymbol{\mu}) = c(\mathbf{v}_D,\mathbf{v},\mathbf{w};\boldsymbol{\mu}) + c(\mathbf{v},\mathbf{v}_D,\mathbf{w};\boldsymbol{\mu}) \tag{2.7}$$

and

$$F_d(\mathbf{w};\boldsymbol{\mu}) = -a(\mathbf{v}_D,\mathbf{w}) - c(\mathbf{v}_D,\mathbf{v}_D,\mathbf{w};\boldsymbol{\mu}), \qquad G(q;\boldsymbol{\mu}) = -b(q,\mathbf{v}_D;\boldsymbol{\mu}) \tag{2.8}$$

are the terms resulting from the lifting of non-homogeneous Dirichlet conditions.

We denote by $V=(H^1_{0,\Gamma_D}(\Omega))^2$, $Q=L^2(\Omega)$ the functional spaces for velocity and pressure, where $H^1_{0,\Gamma_D}(\Omega)=\{v\in H^1(\Omega): v|_{\Gamma_D}=0\}$. We also equip V and Q with the following notions of inner products and norms:

$$\begin{aligned} &\|\cdot\|_V=(\cdot,\cdot)_V^{1/2}, && (\mathbf{v},\mathbf{w})_V=(\mathbf{v},\mathbf{w})_{(H^1(\Omega))^2} && \forall\mathbf{v},\mathbf{w}\in V,\\ &\|\cdot\|_Q=(\cdot,\cdot)_Q^{1/2}, && (p,q)_Q=\nu(\bar{\boldsymbol{\mu}}_p)(p,q)_{L^2(\Omega)} && \forall p,q\in Q, \end{aligned} \tag{2.9}$$

respectively, being $(\mathbf{v},\mathbf{w})_{(H^1(\Omega))^2}=(\nabla\mathbf{v},\nabla\mathbf{w})_{(L^2(\Omega))^2}+(\mathbf{v},\mathbf{w})_{(L^2(\Omega))^2}$ and $\nu(\bar{\boldsymbol{\mu}}_p)$ the kinematic viscosity corresponding to a selected value $\bar{\boldsymbol{\mu}}_p$. Moreover, we recall that the following Poincaré inequality holds:

$$\frac{1}{1+C_p^2}\le\frac{\|\nabla v\|^2_{L^2(\Omega)}}{\|v\|^2_{H^1(\Omega)}}\le 1 \qquad \forall v\in V,\quad H^1_0(\Omega)\subset V\subset H^1(\Omega), \tag{2.10}$$

where $C_p=C_p(\Omega)>0$ denotes the Poincaré constant.

For the sake of the analysis, we also provide a more compact notation. Let us denote by X the product space given by $X=V\times Q$, by $Y(\boldsymbol{\mu})=(\mathbf{v}(\boldsymbol{\mu}),p(\boldsymbol{\mu}))\in X$ and $W=(\mathbf{w},q)$. Thus, the parametrized abstract formulation (2.2) can be rewritten in the following form: find $Y(\boldsymbol{\mu})=(\mathbf{v}(\boldsymbol{\mu}),p(\boldsymbol{\mu}))\in X(\Omega)$ such that

$$A(Y(\boldsymbol{\mu}),W;\boldsymbol{\mu}) + C(Y(\boldsymbol{\mu}),Y(\boldsymbol{\mu}),W;\boldsymbol{\mu}) = \tilde{F}(W;\boldsymbol{\mu}) \quad \forall W\in X \tag{2.11}$$

where

$$\begin{aligned} A(Y,W;\boldsymbol{\mu}) &= \tilde{a}(\mathbf{v},\mathbf{w};\boldsymbol{\mu}) + b(p,\mathbf{w};\boldsymbol{\mu}) + b(q,\mathbf{v};\boldsymbol{\mu}),\\ C(Y,Y,W;\boldsymbol{\mu}) &= c(\mathbf{v},\mathbf{v},\mathbf{w};\boldsymbol{\mu}),\\ \tilde{F}(W;\boldsymbol{\mu}) &= F(\mathbf{w};\boldsymbol{\mu}) + G(q;\boldsymbol{\mu}). \end{aligned} \tag{2.12}$$

3. Well posedness of parametrized formulation

We now recall the assumptions required to ensure the well-posedness of the parametrized formulation (2.11) (or (2.2)); some of these will be automatically inherited also by the full-order and the reduced-order approximations. Moreover, we introduce the *affinity assumption* to be fulfilled by the parametrized forms, in order to ensure an efficient Offline/Online computational splitting.

3.1. Well-posedness analysis

The well-posedness of parametrized NS equations can be analyzed either by extending the theory for linear saddle-point problems to account for the nonlinear terms, or by applying the BRR theory [4,5], valid for a wider class of nonlinear equations. These two approaches can be regarded as generalizations of the *Brezzi theory* and the *Babuška theory*, respectively, to the nonlinear NS case. Here we recall the main results necessary to frame this analysis, which are also useful in view of the RB approximation and the *a posteriori* error estimation.

Recalling our parametrized formulation (2.2), we assume that the bilinear forms $a(\cdot,\cdot;\boldsymbol{\mu}) : V \times V \to \mathbb{R}$ and $b(\cdot,\cdot;\boldsymbol{\mu}) : V \times V \to \mathbb{R}$ are continuous: for any $\boldsymbol{\mu} \in \mathcal{D}$,

$$\gamma_a(\boldsymbol{\mu}) = \sup_{\mathbf{v}\in V}\sup_{\mathbf{w}\in V}\frac{a(\mathbf{v},\mathbf{w};\boldsymbol{\mu})}{\|\mathbf{v}\|_V\|\mathbf{w}\|_V} < +\infty, \quad \gamma_b(\boldsymbol{\mu}) = \sup_{q\in Q}\sup_{\mathbf{w}\in V}\frac{b(q,\mathbf{w};\boldsymbol{\mu})}{\|\mathbf{w}\|_V\|q\|_Q} < +\infty \tag{3.1}$$

and satisfy the following stability assumptions: $a(\cdot,\cdot;\boldsymbol{\mu})$ is coercive over V, *i.e.*

$$\exists\ \alpha^{LB}(\boldsymbol{\mu}) > 0 :\ \alpha(\boldsymbol{\mu}) = \inf_{\mathbf{w}\in V}\frac{a(\mathbf{w},\mathbf{w};\boldsymbol{\mu})}{\|\mathbf{w}\|_V^2} \geq \alpha^{LB}(\boldsymbol{\mu})\ \ \forall\ \boldsymbol{\mu}\in\mathcal{D} \tag{3.2}$$

and $b(\cdot,\cdot;\boldsymbol{\mu})$ is inf-sup stable over $V \times Q$, *i.e.*

$$\exists\ \beta_{Br}^{LB}(\boldsymbol{\mu}) > 0 :\ \beta_{Br}(\boldsymbol{\mu}) = \inf_{q\in Q}\sup_{\mathbf{w}\in X}\frac{b(q,\mathbf{w};\boldsymbol{\mu})}{\|\mathbf{w}\|_V\|q\|_Q} \geq \beta_{Br}^{LB}(\boldsymbol{\mu})\ \ \forall\ \boldsymbol{\mu}\in\mathcal{D}. \tag{3.3}$$

Moreover, thanks to *Hölder* inequality and *Sobolev* embedding theorems (see *e.g.* [30], Chapt. 2, Sect. 1.1), the trilinear form $c(\cdot,\cdot,\cdot;\boldsymbol{\mu}) : V \times V \times V \to \mathbb{R}$ is continuous:

$$\gamma_c(\boldsymbol{\mu}) = \sup_{\mathbf{v}\in V}\sup_{\mathbf{w}\in V}\sup_{\mathbf{z}\in V}\frac{c(\mathbf{v},\mathbf{w},\mathbf{z};\boldsymbol{\mu})}{\|\mathbf{v}\|_V\|\mathbf{w}\|_V\|\mathbf{z}\|_V} < +\infty \quad \forall\ \boldsymbol{\mu}\in\mathcal{D}, \tag{3.4}$$

where the continuity constant $\gamma_c(\boldsymbol{\mu})$ is expressed, in the parametrized case, as

$$\gamma_c(\boldsymbol{\mu}) = \tilde{\rho}^2 M_c(\boldsymbol{\mu}) \leq \rho^2 M_c(\boldsymbol{\mu}); \tag{3.5}$$

$M_c(\boldsymbol{\mu})$ is a function depending on the parametrization; see equation (3.15) for its definition. Here $\rho = \rho(\Omega)$ and $\tilde{\rho} = \tilde{\rho}(\Omega)$ denote the Sobolev embedding constants

$$\rho^2 = \sup_{v\in V}\frac{\|v\|_{L^4(\Omega)}^2}{(\nabla v,\nabla v)_{L^2(\Omega)}}, \qquad \tilde{\rho}^2 = \sup_{v\in V}\frac{\|v\|_{L^4(\Omega)}^2}{(v,v)_{H^1(\Omega)}} \tag{3.6}$$

respectively, being $\|w\|_{L^p(\Omega)} = \left(\int_\Omega |w|^p\right)^{1/p}$. In particular, $\tilde{\rho}^2 \leq \rho^2$ thanks to (2.10).

Under the above assumptions, problem (2.2) admits a solution (see *e.g.* [30], Chapt. 2, Thm. 1.2) in the case $\mathbf{v}_D = \mathbf{0}$; the same conclusion holds in the case $\mathbf{v}_D \neq \mathbf{0}$ by replacing $a(\cdot,\cdot;\boldsymbol{\mu})$ with $\tilde{a}(\cdot,\cdot;\boldsymbol{\mu})$ (see *e.g.* [30], Chapt. 2, Thm. 1.6). Moreover, the solution is also unique under a suitable *small data* assumption. In this way, we can analyze the well-posedness of parametrized steady Navier–Stokes equations by extending the framework developed for parametrized Stokes equations [26], based on the *Brezzi theory* [3].

On the other hand, the more general BRR theory [4, 5] can be applied to state the well-posedness of the parametrized formulation (2.11). As the *Babuška theory* for mixed variational problems, it is based on the global operator $\tilde{A}(\cdot,\cdot;\boldsymbol{\mu}) : X \times X \to \mathbb{R}$, defined in our case by

$$\tilde{A}(U,W;\boldsymbol{\mu}) = A(U,W;\boldsymbol{\mu}) + C(U,U,W;\boldsymbol{\mu}). \tag{3.7}$$

Here $A(\cdot,\cdot;\boldsymbol{\mu})$ and $C(\cdot,\cdot,\cdot;\boldsymbol{\mu})$ denote the operators defined in (2.12). Moreover, we denote by

$$\mathrm{d}\tilde{A}(Y;\boldsymbol{\mu})(U,W) = A(U,W;\boldsymbol{\mu}) + C(Y,U,W;\boldsymbol{\mu}) + C(U,Y,W;\boldsymbol{\mu}) \tag{3.8}$$

the Fréchet derivative of $\tilde{A}(\cdot,\cdot;\boldsymbol{\mu})$ with respect to the first variable. According to the BRR theory, problem (2.11) admits a solution if and only if the following continuity condition:

$$\gamma(\boldsymbol{\mu}) = \sup_{U\in X}\sup_{W\in X}\frac{\mathrm{d}\tilde{A}(Y(\boldsymbol{\mu});\boldsymbol{\mu})(U,W)}{\|U\|_X\|W\|_X} < +\infty, \quad \forall\ \boldsymbol{\mu}\in\mathcal{D}, \tag{3.9}$$

and the following (Babuška) inf-sup condition:

$$\exists\ \beta^{LB}(\boldsymbol{\mu}) > 0 :\ \beta(\boldsymbol{\mu}) = \inf_{U\in X}\sup_{W\in X}\frac{\mathrm{d}\tilde{A}(Y(\boldsymbol{\mu});\boldsymbol{\mu})(U,W)}{\|U\|_X\|W\|_X} \geq \beta^{LB}(\boldsymbol{\mu}) \quad \forall\ \boldsymbol{\mu}\in\mathcal{D} \tag{3.10}$$

hold. Moreover, the solution in a neighborhood of $Y(\boldsymbol{\mu})$ is unique. Besides the well-posedness analysis, this framework will be exploited in Section 6 also to derive an *a posteriori* error bound for the RB approximation.

3.2. Affine and nonaffine parametric dependence

In order to develop an Offline/Online computational procedure, we require that the forms (2.3)–(2.4) fulfill the assumption of affine parametric dependence. In our case, provided the physical parametrizations depend just on $\boldsymbol{\mu}_p$ but not on the spatial coordinates $\mathbf{x}$, if the transformation maps $T^k(\cdot;\boldsymbol{\mu}_g)$ are affine, the parametrized tensor (2.5)–(2.6) depend just on $\boldsymbol{\mu}$. In this way the bilinear forms (2.3) can be written, for some $Q_a, Q_b > 0$, as:

$$a(\mathbf{v},\mathbf{w};\boldsymbol{\mu}) = \sum_{q=1}^{Q_a}\Theta_a^q(\boldsymbol{\mu})\,a^q(\mathbf{v},\mathbf{w}), \qquad b(q,\mathbf{w};\boldsymbol{\mu}) = \sum_{q=1}^{Q_b}\Theta_b^q(\boldsymbol{\mu})b^q(q,\mathbf{w}); \tag{3.11}$$

where q is a condensed index of i,j,k quantities and, for $1\leq k\leq K_{\mathrm{dom}}$, $1\leq i,j\leq 2$,

$$\Theta_a^{q(i,j,k)}(\boldsymbol{\mu}) = \kappa_{ij}^k(\boldsymbol{\mu}), \qquad a^{q(i,j,k)}(\mathbf{v},\mathbf{w}) = \int_{\Omega^k}\frac{\partial\mathbf{v}}{\partial x_i}\frac{\partial\mathbf{w}}{\partial x_j}\mathrm{d}\Omega, \tag{3.12}$$

$$\Theta_b^{q(i,j,k)}(\boldsymbol{\mu}) = \chi_{ij}^k(\boldsymbol{\mu}), \qquad b^{q(i,j,k)}(q,\mathbf{w}) = -\int_{\Omega^k} q\frac{\partial w_i}{\partial x_j}\mathrm{d}\Omega. \tag{3.13}$$

For the trilinear form and the source term (*e.g.* in the case $\mathbf{g}^N = \mathbf{0}$), we have instead:

$$c(\mathbf{v},\mathbf{w},\mathbf{z};\boldsymbol{\mu}) = \sum_{q=1}^{Q_c}\Theta_c^q(\boldsymbol{\mu})c^q(\mathbf{v},\mathbf{w},\mathbf{z}), \qquad F_s(\mathbf{w};\boldsymbol{\mu}) = \sum_{q'=1}^{Q_s}\Theta_s^{q'}(\boldsymbol{\mu})F_s^{q'}(\mathbf{w}), \tag{3.14}$$

for some $Q_c, Q_s > 0$, where q and q' are condensed indexes of (i,j,k) and k quantities, respectively, and

$$\Theta_c^{q(i,j,k)}(\boldsymbol{\mu}) = \chi_{ji}^k(\boldsymbol{\mu}), \qquad c^{q(i,j,k)}(\mathbf{v},\mathbf{w},\mathbf{z}) = \int_{\Omega^k} v_i\frac{\partial w_k}{\partial x_j}z_k\ \mathrm{d}\Omega,$$

$$\Theta_s^{q'(k)}(\boldsymbol{\mu}) = |J_T^k(\cdot;\boldsymbol{\mu})|, \qquad F_s^{q'(k)}(\mathbf{w}) = \int_{\Omega^k}\mathbf{f}\cdot\mathbf{w}\mathrm{d}\Omega.$$

On the other hand, if the parametric maps $T^k(\cdot;\boldsymbol{\mu}_g)$ are nonaffine, parametrized tensors are function of both spatial coordinates $\mathbf{x}$ and parameter $\boldsymbol{\mu}$. In this case we rely on the EIM (see *e.g.* [1,17]) in order to recover the affinity assumption. If we assume, *e.g.*, to deal with a global map ($K_{\text{dom}} = 1$), each component of the tensors $\boldsymbol{\kappa}$ and $\boldsymbol{\chi}$ has to be approximated by an affine expansion:

$$\kappa_{ij}(\mathbf{x},\boldsymbol{\mu}) = \sum_{k=1}^{K_{ij}^a} \beta_k^{i,j}(\boldsymbol{\mu})\xi_k^{i,j}(\mathbf{x}) + \varepsilon_{i,j}^a(\mathbf{x};\boldsymbol{\mu}), \quad \chi_{ij}(\mathbf{x},\boldsymbol{\mu}) = \sum_{k=1}^{K_{ij}^b} \gamma_k^{i,j}(\boldsymbol{\mu})\eta_k^{i,j}(\mathbf{x}) + \varepsilon_{i,j}^b(\mathbf{x};\boldsymbol{\mu}), \tag{3.15}$$

for $1 \le i,j \le 2$, where K_{ij}^a and K_{ij}^b represent the total number of terms obtained for each tensorial component through EIM. In particular, we denote by $M_c(\boldsymbol{\mu}) = \sqrt{2}\max_{q=1,\dots,Q_c} \|\Theta_q^c(\boldsymbol{\mu})\|_{L^\infty(\mathcal{D})} \max_{q=1,\dots,Q_c} \|\eta^q\|_{L^\infty(\Omega)}$, where η^q is defined in (3.15) – q is a condensed index of i,j,k – and it is such that $\eta^q = 1$ in the affine case.

The same expansion (made now by K^s terms) is set up for the tensor appearing at the right-hand-side of velocity equation:

$$|\det(J_T(\mathbf{x};\boldsymbol{\mu}))| = \sum_{k=1}^{K^s} \delta_k(\boldsymbol{\mu})\psi_k(\mathbf{x}) + \varepsilon^s(\mathbf{x};\boldsymbol{\mu}). \tag{3.16}$$

All the coefficients $\beta_k^{i,j}$'s, $\gamma_k^{i,j}$'s, δ_k's, $\xi_k^{i,j}$'s, $\eta_k^{i,j}$'s and ψ_k's are efficiently computable scalar functions and the error terms are guaranteed to be under some prescribed tolerance:

$$\|\varepsilon_{i,j}^{(a,b)}(\cdot;\boldsymbol{\mu})\|_\infty \le \varepsilon_{tol}^{EIM}, \qquad \|\varepsilon^s(\cdot;\boldsymbol{\mu})\|_\infty \le \varepsilon_{tol}^{EIM} \qquad \forall \boldsymbol{\mu} \in \mathcal{D}.$$

In this way, we can recover the affine expansions (3.11)–(3.14) by setting

$$a^{q(i,j,k)}(\mathbf{v},\mathbf{w}) = \int_\Omega \xi_k^{i,j}(\mathbf{x})\frac{\partial \mathbf{v}}{\partial x_i}\frac{\partial \mathbf{w}}{\partial x_j}, \qquad b^{q(i,j,k)}(p,\mathbf{w}) = -\int_\Omega \eta_k^{i,j}(\mathbf{x})p\frac{\partial \mathbf{w}_i}{\partial x_j},$$
$$c^{q(i,j,k)}(\mathbf{v},\mathbf{w},\mathbf{z}) = \int_{\Omega^k} v_i\eta_k^{i,j}(\mathbf{x})\frac{\partial w_k}{\partial x_j}z_k, \qquad F_s^{q(k)}(\mathbf{w}) = \int_{\Omega^k} \psi_k(\mathbf{x})\mathbf{f}\cdot\mathbf{w},$$

with $\Theta_a^q(\boldsymbol{\mu}) = \beta_k^{i,j}(\boldsymbol{\mu})$, $\Theta_b^q(\boldsymbol{\mu}) = \Theta_c^q(\boldsymbol{\mu}) = \gamma_k^{i,j}(\boldsymbol{\mu})$, $\Theta_s^q(\boldsymbol{\mu}) = \delta_k(\boldsymbol{\mu})$. Thus, we can express all the operators appearing in (2.2) as linear combinations of parameter-independent forms through some weights given by real functions of the parameters.

4. Truth approximation: Stability and algebraic formulation

We briefly recall the main features related to the FE truth approximation, over which the RB approximation is built, as well the conditions ensuring its stability. We also build the algebraic version of the truth approximation, since it is required later on to set the corresponding structures for the RB approximation.

4.1. Formulation and stability

Let $V^{\mathcal{N}} \subset V$ and $Q^{\mathcal{N}} \subset Q$ be two subspaces of V and Q, of dimension $\mathcal{N}_V, \mathcal{N}_Q < +\infty$, respectively, and let us denote by $\mathbf{v}^{\mathcal{N}}(\boldsymbol{\mu}) \in V^{\mathcal{N}}$ and $p^{\mathcal{N}}(\boldsymbol{\mu}) \in Q^{\mathcal{N}}$ the FE approximations for the velocity and the pressure fields [25]. We suppose that the dimension of the FE spaces is large enough that the differences $\|\mathbf{v}^{\mathcal{N}}(\boldsymbol{\mu}) - \mathbf{v}(\boldsymbol{\mu})\|_V$, $\|p^{\mathcal{N}}(\boldsymbol{\mu}) - p(\boldsymbol{\mu})\|_Q$ can be neglected – in other words, it can be effectively considered as a "truth" approximation. Moreover, (2.9) defines our inner product and norm for members of $V^{\mathcal{N}} \subset V$ and $Q^{\mathcal{N}} \subset Q$, respectively.

We can now introduce the Galerkin-FE approximation of the parametrized problem (2.11) (or (2.2)): given $\boldsymbol{\mu} \in \mathcal{D}$, we seek for $Y^{\mathcal{N}}(\boldsymbol{\mu}) = (\mathbf{v}^{\mathcal{N}}(\boldsymbol{\mu}), p^{\mathcal{N}}(\boldsymbol{\mu})) \in X^{\mathcal{N}} := V^{\mathcal{N}} \times Q^{\mathcal{N}}$ such that

$$A\left(Y^{\mathcal{N}}(\boldsymbol{\mu}), W^{\mathcal{N}};\boldsymbol{\mu}\right) + C\left(Y^{\mathcal{N}}(\boldsymbol{\mu}), Y^{\mathcal{N}}(\boldsymbol{\mu}), W^{\mathcal{N}};\boldsymbol{\mu}\right) = \tilde{F}\left(W^{\mathcal{N}};\boldsymbol{\mu}\right) \quad \forall W^{\mathcal{N}} \in X^{\mathcal{N}} \tag{4.1}$$

or, equivalently,

$$\begin{cases} \tilde{a}\left(\mathbf{v}^{\mathcal{N}}(\boldsymbol{\mu}), \mathbf{w}^{\mathcal{N}}; \boldsymbol{\mu}\right) + b\left(p^{\mathcal{N}}(\boldsymbol{\mu}), \mathbf{w}^{\mathcal{N}}; \boldsymbol{\mu}\right) + c\left(\mathbf{v}^{\mathcal{N}}(\boldsymbol{\mu}), \mathbf{v}^{\mathcal{N}}(\boldsymbol{\mu}), \mathbf{w}^{\mathcal{N}}; \boldsymbol{\mu}\right) = F\left(\mathbf{w}^{\mathcal{N}}; \boldsymbol{\mu}\right) & \forall \mathbf{w}^{\mathcal{N}} \in V^{\mathcal{N}} \\ b\left(q^{\mathcal{N}}, \mathbf{v}^{\mathcal{N}}(\boldsymbol{\mu}); \boldsymbol{\mu}\right) = G\left(q^{\mathcal{N}}; \boldsymbol{\mu}\right) & \forall q^{\mathcal{N}} \in Q^{\mathcal{N}}. \end{cases} \tag{4.2}$$

All the forms are continuous over the discrete spaces $V^{\mathcal{N}}$ and $Q^{\mathcal{N}}$. In particular, a discrete version of the Sobolev embedding result can be stated (see *e.g.* [30]), where

$$\rho_{\mathcal{N}}^2 = \sup_{v \in V^{\mathcal{N}}} \frac{\|v\|_{L^4(\Omega)}^2}{(\nabla v, \nabla v)_{L^2(\Omega)}}, \qquad \rho_{V,\mathcal{N}}^2 = \sup_{v \in V^{\mathcal{N}}} \frac{\|v\|_{L^4(\Omega)}^2}{(v, v)_{H^1(\Omega)}} \tag{4.3}$$

are the discrete versions of the Sobolev constants in (3.6). Conversely, the approximation stability is ensured by imposing that the coercivity and inf-sup conditions are still valid at the discrete level. In particular, $a(\cdot, \cdot; \boldsymbol{\mu})$ is automatically coercive over $V^{\mathcal{N}}$:

$$\exists\, \alpha_{\mathcal{N}}^{LB}(\boldsymbol{\mu}) > 0 : \ \alpha^{\mathcal{N}}(\boldsymbol{\mu}) = \inf_{\mathbf{v} \in V^{\mathcal{N}}} \frac{a(\mathbf{v}, \mathbf{v}; \boldsymbol{\mu})}{\|\mathbf{v}\|_V^2} \geq \alpha_{\mathcal{N}}^{LB}(\boldsymbol{\mu}) \quad \forall\, \boldsymbol{\mu} \in \mathcal{D}. \tag{4.4}$$

On the other hand, we require that $b(\cdot, \cdot; \boldsymbol{\mu})$ is inf-sup stable over $V^{\mathcal{N}} \times Q^{\mathcal{N}}$, so that the following discrete Brezzi inf-sup condition [3]:

$$\exists\, \beta_{Br,\mathcal{N}}^{LB}(\boldsymbol{\mu}) > 0 : \ \beta_{Br,\mathcal{N}}(\boldsymbol{\mu}) = \inf_{q \in Q^{\mathcal{N}}} \sup_{\mathbf{w} \in V^{\mathcal{N}}} \frac{b(q, \mathbf{w}; \boldsymbol{\mu})}{\|\mathbf{w}\|_V \|q\|_Q} \geq \beta_{Br,\mathcal{N}}^{LB}(\boldsymbol{\mu}) \quad \forall\, \boldsymbol{\mu} \in \mathcal{D} \tag{4.5}$$

holds. This last property is ensured *e.g.* by choosing $V^{\mathcal{N}} \times Q^{\mathcal{N}}$ as the space of Taylor–Hood $\mathbb{P}_2 - \mathbb{P}_1$ elements [11]; however, this choice is not restrictive – the whole construction keeps holding for other spaces combinations as well. We also introduce the (inner, pressure) supremizer operator $T_p^{\boldsymbol{\mu}}$: $Q^{\mathcal{N}} \to V^{\mathcal{N}}$, defined as

$$(T_p^{\boldsymbol{\mu}} q, \mathbf{w})_V = b(q, \mathbf{w}; \boldsymbol{\mu}) \quad \forall\, \mathbf{w} \in V^{\mathcal{N}}, \tag{4.6}$$

so that we can express the inf-sup condition (4.5) as (see *e.g.* [26,28])

$$T_p^{\boldsymbol{\mu}} q = \arg \sup_{\mathbf{w} \in V^{\mathcal{N}}} \frac{b(q, \mathbf{w}; \boldsymbol{\mu})}{\|\mathbf{w}\|_V} \qquad \text{and} \qquad (\beta_{Br,\mathcal{N}}(\boldsymbol{\mu}))^2 = \inf_{q \in Q^{\mathcal{N}}} \frac{(T_p^{\boldsymbol{\mu}} q, T_p^{\boldsymbol{\mu}} q)_V}{\|q\|_Q^2}. \tag{4.7}$$

This operator will play a fundamental role in the stability of the RB approximation, as we will see in Section 5. Furthermore, (4.2) admits a solution in the case of homogeneous Dirichlet conditions if (4.4) and (4.5) hold. As before, in the case of inhomogeneous Dirichlet conditions, we need to replace $a(\cdot, \cdot; \boldsymbol{\mu})$ with $\tilde{a}(\cdot, \cdot; \boldsymbol{\mu})$. Moreover, by defining $\gamma_c^{\mathcal{N}}(\boldsymbol{\mu}) = \rho_{V,\mathcal{N}}^2 M_c(\boldsymbol{\mu}) \leq \rho_{\mathcal{N}}^2 M_c(\boldsymbol{\mu})$, uniqueness is ensured by the following *small data* assumption:

$$\frac{4\, \gamma_c^{\mathcal{N}}(\boldsymbol{\mu})}{\left(\alpha_{\mathcal{N}}^{LB}(\boldsymbol{\mu})\right)^2} \|F(\cdot; \boldsymbol{\mu})\|_{(H^{-1}(\Omega))^2} < 1. \tag{4.8}$$

In the same way as for the continuous level, the BRR theory provides a more general framework to state the well-posedness of the finite dimensional approximation (2.11). We remark that the discrete version of continuity and inf-sup stability conditions (3.9)–(3.10) reads as follows: for all $\boldsymbol{\mu} \in \mathcal{D}$,

$$\gamma_{\mathcal{N}}(\boldsymbol{\mu}) = \sup_{U \in X^{\mathcal{N}}} \sup_{W \in X^{\mathcal{N}}} \frac{\mathrm{d}\tilde{A}\left(Y^{\mathcal{N}}(\boldsymbol{\mu}); \boldsymbol{\mu}\right)(U, W)}{\|U\|_X \|W\|_X} < +\infty \tag{4.9}$$

$$\exists\, \beta_{\mathcal{N}}^{LB}(\boldsymbol{\mu}) > 0 : \ \beta_{\mathcal{N}}(\boldsymbol{\mu}) = \inf_{U \in X^{\mathcal{N}}} \sup_{W \in X^{\mathcal{N}}} \frac{\mathrm{d}\tilde{A}\left(Y^{\mathcal{N}}(\boldsymbol{\mu}); \boldsymbol{\mu}\right)(U, W)}{\|U\|_X \|W\|_X} \geq \beta_{\mathcal{N}}^{LB}(\boldsymbol{\mu}). \tag{4.10}$$

4.2. Algebraic formulation of the FE truth approximation

We can now derive the matrix formulation corresponding to the Galerkin-FE approximation (4.2); this constitutes an essential ingredient in order to build our RB approximation in the following. Let us denote by $\{\boldsymbol{\phi}_i^{\mathbf{v}}\}_{i=1}^{\mathcal{N}_V}$ and $\{\phi_i^p\}_{i=1}^{\mathcal{N}_Q}$ the Lagrangian basis of the FE spaces $V^{\mathcal{N}}$ and $Q^{\mathcal{N}}$, respectively, so that we can express the FE velocity and pressure as

$$\mathbf{v}^{\mathcal{N}}(\boldsymbol{\mu}) = \sum_{i=1}^{\mathcal{N}_V} u_i^{\mathcal{N}}(\boldsymbol{\mu})\boldsymbol{\phi}_i^{\mathbf{v}}, \qquad p^{\mathcal{N}}(\boldsymbol{\mu}) = \sum_{i=1}^{\mathcal{N}_Q} p_i^{\mathcal{N}}(\boldsymbol{\mu})\phi_i^p. \tag{4.11}$$

We remark that the solution to (4.1) is vanishing on the whole Dirichlet boundary, so that the corresponding velocity approximation fulfilling the boundary conditions is given by $\mathbf{v}^{\mathcal{N}}(\boldsymbol{\mu}) + \mathbf{v}_D^{\mathcal{N}}$, being $\mathbf{v}_D^{\mathcal{N}} \in V^{\mathcal{N}}$ a discrete function interpolating Dirichlet data. Thus, by denoting as $\underline{\mathbf{v}}_{\mathcal{N}}(\boldsymbol{\mu}) \in \mathbb{R}^{\mathcal{N}_V}$ and $\underline{\mathbf{p}}_{\mathcal{N}}(\boldsymbol{\mu}) \in \mathbb{R}^{\mathcal{N}_Q}$ the vectors of the degrees of freedom appearing in (4.11), problem (4.2) can be rewritten as:

$$\begin{bmatrix} \mathbb{A}_{\mathcal{N}}(\boldsymbol{\mu}) + \mathbb{D}_{\mathcal{N}}(\boldsymbol{\mu}) + \mathbb{C}_{\mathcal{N}}(\underline{\mathbf{v}}_{\mathcal{N}}(\boldsymbol{\mu}); \boldsymbol{\mu}) & \mathbb{B}_{\mathcal{N}}^T(\boldsymbol{\mu}) \\ \mathbb{B}_{\mathcal{N}}(\boldsymbol{\mu}) & 0 \end{bmatrix} \begin{bmatrix} \underline{\mathbf{v}}_{\mathcal{N}}(\boldsymbol{\mu}) \\ \underline{\mathbf{p}}_{\mathcal{N}}(\boldsymbol{\mu}) \end{bmatrix} = \begin{bmatrix} \mathbf{f}_{\mathcal{N}}(\boldsymbol{\mu}) \\ \mathbf{g}_{\mathcal{N}}(\boldsymbol{\mu}) \end{bmatrix} \tag{4.12}$$

where, for $1 \le i, j \le \mathcal{N}_V$ and $1 \le k \le \mathcal{N}_Q$,

$$\begin{aligned} (\mathbb{A}_{\mathcal{N}}(\boldsymbol{\mu}))_{ij} &= a\left(\boldsymbol{\phi}_j^{\mathbf{v}}, \boldsymbol{\phi}_i^{\mathbf{v}}; \boldsymbol{\mu}\right), \qquad (\mathbb{B}_{\mathcal{N}}(\boldsymbol{\mu}))_{ki} = b\left(\phi_k^p, \boldsymbol{\phi}_i^{\mathbf{v}}; \boldsymbol{\mu}\right), \\ (\mathbb{C}_{\mathcal{N}}(\underline{\mathbf{w}}; \boldsymbol{\mu})_{\mathcal{N}})_{ij} &= \sum_{m=1}^{\mathcal{N}_V} w_m^{\mathcal{N}} c\left(\boldsymbol{\phi}_m^{\mathbf{v}}, \boldsymbol{\phi}_j^{\mathbf{v}}, \boldsymbol{\phi}_i^{\mathbf{v}}; \boldsymbol{\mu}\right), \end{aligned} \tag{4.13}$$

$$\begin{aligned} (\mathbb{D}_{\mathcal{N}}(\boldsymbol{\mu}))_{ij} &= d\left(\boldsymbol{\phi}_j^{\mathbf{v}}, \boldsymbol{\phi}_i^{\mathbf{v}}; \boldsymbol{\mu}\right), \qquad (\mathbf{g}_{\mathcal{N}}(\boldsymbol{\mu}))_k = -b\left(\phi_k^p, \mathbf{v}_D^{\mathcal{N}}; \boldsymbol{\mu}\right), \\ (\mathbf{f}_{\mathcal{N}}(\boldsymbol{\mu}))_i &= F_s\left(\boldsymbol{\phi}_i^{\mathbf{v}}; \boldsymbol{\mu}\right) - a\left(\mathbf{v}_D^{\mathcal{N}}, \boldsymbol{\phi}_i^{\mathbf{v}}; \boldsymbol{\mu}\right) - c\left(\mathbf{v}_D^{\mathcal{N}}, \mathbf{v}_D^{\mathcal{N}}, \boldsymbol{\phi}_i^{\mathbf{v}}; \boldsymbol{\mu}\right). \end{aligned} \tag{4.14}$$

We solve the nonlinear saddle-point problem (4.12) by means of a *fixed-point iteration* since, relative to a Newton iteration, it has a *huge* ball of convergence (see *e.g.* [9], Chapt. 7.2 and references therein). Moreover, if the *small data* condition (4.8) is satisfied, the fixed-point method is *globally* convergent. Thus, starting from an initial guess $(\underline{\mathbf{v}}_{\mathcal{N}}^{(0)}(\boldsymbol{\mu}), \underline{\mathbf{p}}_{\mathcal{N}}^{(0)}(\boldsymbol{\mu}))$, for $k \ge 1$ we solve

$$\begin{bmatrix} \mathbb{A}_{\mathcal{N}}(\boldsymbol{\mu}) + \mathbb{D}_{\mathcal{N}}(\boldsymbol{\mu}) + \mathbb{C}_{\mathcal{N}}(\underline{\mathbf{v}}_{\mathcal{N}}^{(k-1)}(\boldsymbol{\mu}); \boldsymbol{\mu}) & \mathbb{B}_{\mathcal{N}}^T(\boldsymbol{\mu}) \\ \mathbb{B}_{\mathcal{N}}(\boldsymbol{\mu}) & 0 \end{bmatrix} \begin{bmatrix} \underline{\mathbf{v}}_{\mathcal{N}}^{(k)}(\boldsymbol{\mu}) \\ \underline{\mathbf{p}}_{\mathcal{N}}^{(k)}(\boldsymbol{\mu}) \end{bmatrix} = \begin{bmatrix} \mathbf{f}_{\mathcal{N}}(\boldsymbol{\mu}) \\ \mathbf{g}_{\mathcal{N}}(\boldsymbol{\mu}) \end{bmatrix}, \tag{4.15}$$

to obtain $(\underline{\mathbf{v}}_{\mathcal{N}}^{(k)}(\boldsymbol{\mu}), \underline{\mathbf{p}}_{\mathcal{N}}^{(k)}(\boldsymbol{\mu}))$, until $\|\mathbf{v}_{\mathcal{N}}^{(k)}(\boldsymbol{\mu}) - \mathbf{v}_{\mathcal{N}}^{(k-1)}(\boldsymbol{\mu})\|_V \le \varepsilon_{\text{tol}}^{NS}$, given a small tolerance $\varepsilon_{\text{tol}}^{NS} > 0$. As initial guess, we take the Stokes solution of (4.12). Each Oseen system (4.15) is solved by means of a *sparse* LU factorization; different approaches for solving (4.12) are based on the use of *homotopy/continuation* with respect to the parameters, whenever interested in one solution branch, as shown in [7].

5. Reduced Basis approximation of parametrized Navier–Stokes equations

We now present the main components of the RB approximation for parametrized Navier–Stokes equations – namely, a Galerkin projection onto a low-dimensional space, built through a greedy procedure [24,27]; an efficient Offline/Online splitting; and a sharp (yet inexpensive) *a posteriori* error estimation. The characterization of these ingredients in the case of Navier–Stokes equations is the goal of this section and the following one. In particular, after showing the construction of stable RB spaces, we deduce the algebraic formulation of the RB problem, as well as an efficient way to manage the storing of algebraic structures related to nonlinear terms.

Given a positive integer $N_{\max}$, let us introduce a sequence of (hierarchical[3]) approximation spaces: for $N = 1, \dots, N_{\max}$, $V_N \subset V^{\mathcal{N}}$ and $Q_N \subset Q^{\mathcal{N}}$ are N-dimensional subspaces of $V^{\mathcal{N}}$ and $Q^{\mathcal{N}}$, respectively, where typically $N \ll \mathcal{N}$.

The RB approximation $(\mathbf{v}_N(\boldsymbol{\mu}), p_N(\boldsymbol{\mu}))$ of velocity and pressure fields, respectively, can be obtained by means of a Galerkin projection onto the reduced spaces $V_N \times Q_N$ as follows: given $\boldsymbol{\mu} \in \mathcal{D}$, find $Y_N(\boldsymbol{\mu}) = (\mathbf{v}_N(\boldsymbol{\mu}), p_N(\boldsymbol{\mu})) \in X_N := V_N \times Q_N$ such that

$$A(Y_N(\boldsymbol{\mu}), W_N; \boldsymbol{\mu}) + C(Y_N(\boldsymbol{\mu}), Y_N(\boldsymbol{\mu}), W_N; \boldsymbol{\mu}) = \tilde{F}(W_N; \boldsymbol{\mu}) \quad \forall W_N \in X_N \tag{5.1}$$

or, equivalently,

$$\begin{cases} \tilde{a}(\mathbf{v}_N(\boldsymbol{\mu}), \mathbf{w}_N; \boldsymbol{\mu}) + b(p_N(\boldsymbol{\mu}), \mathbf{w}_N; \boldsymbol{\mu}) + c(\mathbf{v}_N(\boldsymbol{\mu}), \mathbf{v}_N(\boldsymbol{\mu}), \mathbf{w}_N; \boldsymbol{\mu}) = F(\mathbf{w}_N; \boldsymbol{\mu}) & \forall \mathbf{w}_N \in V_N \\ b(q_N, \mathbf{v}_N(\boldsymbol{\mu}); \boldsymbol{\mu}) = G(q_N; \boldsymbol{\mu}) & \forall q_N \in Q_N. \end{cases} \tag{5.2}$$

In the following subsection we extend to the NS case the construction of *stable* RB spaces – *i.e.*, spaces which fulfill the (Brezzi) inf-sup condition stability, by enriching the velocity space with the solutions of the supremizer problem (4.6) – and briefly discuss the well-posedness of the RB approximation (5.1) (or (5.2)).

5.1. Construction of RB spaces and inf-sup stability

The reduced space $X_N = V_N \times Q_N$ is a global approximation space made up of well-chosen solutions (or snapshots) $(\mathbf{v}^{\mathcal{N}}(\boldsymbol{\mu}^1), p^{\mathcal{N}}(\boldsymbol{\mu}^1)), \dots, (\mathbf{v}^{\mathcal{N}}(\boldsymbol{\mu}^N), p^{\mathcal{N}}(\boldsymbol{\mu}^N))$. To build this space, we rely on a standard greedy algorithm (see *e.g.* [24,27]), driven by an *a posteriori* error bound $\Delta_N(\boldsymbol{\mu})$, such that $\|Y^{\mathcal{N}}(\boldsymbol{\mu}) - Y_N(\boldsymbol{\mu})\|_X \leq \Delta_N(\boldsymbol{\mu})$ for all $\boldsymbol{\mu} \in \mathcal{D}$. Thus, starting from a given parameter value $\boldsymbol{\mu}^1$ and the corresponding snapshot $(\mathbf{v}^{\mathcal{N}}(\boldsymbol{\mu}^1), p^{\mathcal{N}}(\boldsymbol{\mu}^1))$, we iteratively build the set $S_N = \{\boldsymbol{\mu}^1, \dots, \boldsymbol{\mu}^N\}$ by selecting, at the $(n+1)$-th iteration of the algorithm,

$$\boldsymbol{\mu}^{n+1} = \arg \max_{\boldsymbol{\mu} \in \Xi_{\text{train}}} \Delta_n(\boldsymbol{\mu}),$$

and adding to the reduced space the corresponding snapshot $(\mathbf{v}^{\mathcal{N}}(\boldsymbol{\mu}^n), p^{\mathcal{N}}(\boldsymbol{\mu}^n))$. In other words, at each iteration we select, over all possible $(\mathbf{v}^{\mathcal{N}}(\boldsymbol{\mu}), p^{\mathcal{N}}(\boldsymbol{\mu}))$, $\boldsymbol{\mu} \in \Xi_{\text{train}}$, the snapshot that the *a posteriori* error bound $\Delta_n(\boldsymbol{\mu})$ predicts to be worst approximated by the RB approximation associated to the $n-1$ snapshots already retained. Here Ξ_{train} is a train sample which serves to select the RB space. The procedure stops at that step $N = N_{\max}$ for which $\Delta_N(\boldsymbol{\mu}) \leq \varepsilon_{\text{tol}}^{\text{RB}}$ $\forall \boldsymbol{\mu} \in \Xi_{\text{train}}$, being $\varepsilon_{\text{tol}}^{\text{RB}}$ a prescribed positive tolerance.

Nevertheless, a further step is required in order to guarantee the inf-sup stability of the RB approximation. To this aim, we define the *reduced basis pressure space* $Q_N \subset Q^{\mathcal{N}}$ as

$$Q_N = \text{span}\left\{\tilde{\zeta}_n^p := p^{\mathcal{N}}(\boldsymbol{\mu}^n),\ n = 1, \dots, N\right\}, \qquad N = 1, \dots N_{\max}. \tag{5.3}$$

The *reduced basis velocity space* $V_N \subset V^{\mathcal{N}}$ can be built as

$$V_N = \text{span}\left\{\tilde{\boldsymbol{\zeta}}_n^{\mathbf{v}} := \mathbf{v}^{\mathcal{N}}(\boldsymbol{\mu}^n),\ T_p^{\boldsymbol{\mu}} \tilde{\zeta}_n^p,\ n = 1, \dots, N\right\}, \qquad N = 1, \dots N_{\max}, \tag{5.4}$$

thus enriching the space of velocity snapshots with the inner (pressure) supremizers.

Thanks to these definitions, problem (5.2) fulfills an equivalent Brezzi RB inf-sup condition. In fact, by defining the RB stability factor as

$$\beta_{Br,N}(\boldsymbol{\mu}) = \inf_{q \in Q_N} \sup_{\mathbf{w} \in V_N} \frac{b(q, \mathbf{w}; \boldsymbol{\mu})}{\|\mathbf{w}\|_V \|q\|_Q} \tag{5.5}$$

[3]In other words, $V_1 \subset V_2 \subset \dots \subset V_{N_{\max}}$ and $Q_1 \subset Q_2 \subset \dots \subset Q_{N_{\max}}$. This condition is important in order to ensure an efficient storing of RB structures, and thus a rapid Online evaluation.

the following inequalities hold (see *e.g.* [28] for the proof):

$$\beta_{Br,N}(\boldsymbol{\mu}) \geq \beta_{Br,\mathcal{N}}(\boldsymbol{\mu}) > 0 \qquad \forall\, \boldsymbol{\mu} \in \mathcal{D}, \tag{5.6}$$

where $\beta_{Br,\mathcal{N}}(\boldsymbol{\mu})$ is defined in (4.5). We point out that, since the coercivity of the bilinear form $a(\cdot\,\cdot;\boldsymbol{\mu})$ – respectively, $\tilde{a}(\cdot,\cdot;\boldsymbol{\mu})$ – is still fulfilled on the reduced velocity space $V_N \subset V^{\mathcal{N}}$, the RB solution is stable in the sense of the Brezzi inf-sup condition thanks to (5.6). Uniqueness of the RB solution will be discussed in Section 6, where we also provide an error estimate for both RB velocity and pressure.

We also remark that, by enriching the velocity space[4] with the supremizers $T_p^{\boldsymbol{\mu}}\tilde{\zeta}_n^p$, for $n = 1, \dots N$, the RB velocity space (5.4) has dimension $2N$, the double of the dimension N of the RB pressure space. Finally, we introduce two orthonormal basis of the RB spaces Q_N and V_N, denoted by $\{\zeta_n^p\}_{n=1}^N$ and $\{\boldsymbol{\zeta}_n^{\mathbf{v}}\}_{n=1}^{2N}$, respectively. We exploit the Gram-Schmidt orthonormalization procedure to orthonormalize the snapshots; see *e.g.* [17,28] for further details related to its formulation for this kind of spaces. Similarly, we can express the supremizer solutions in (5.4) in a more efficient way, as in the RB approximation of a Stokes problem, for which a detailed analysis is reported in [26].

We close this section by underlining an important feature of the RB framework presented in this paper. As we will see in Section 6, the *a posteriori* error bound requires the calculation of the stability factor $\beta_{\mathcal{N}}(\boldsymbol{\mu})$ defined in (4.10). Compared to RB methods for NS equations proposed in the literature (see *e.g.* [7,8]), a remarkable novelty of our approach is the possibility to decouple the generation of the reduced spaces from the calculation of stability factors. Although the former still exploits the *a posteriori* error bound (like in [7,8]), the latter can be performed before computing the FE snapshots, for the sake of computational savings.

5.2. Algebraic formulation of the RB approximation

We now show how the RB approximation (5.2) can be easily formulated in algebraic terms. In fact, by expressing the RB solution as a combination of the basis functions:

$$\mathbf{v}_N(\boldsymbol{\mu}) = \sum_{j=1}^{2N} v_{Nj}(\boldsymbol{\mu})\boldsymbol{\zeta}_j^{\mathbf{v}}, \qquad p_N(\boldsymbol{\mu}) = \sum_{l=1}^{N} p_{Nl}(\boldsymbol{\mu})\zeta_l^p,$$

we have that the weights $\underline{\mathbf{v}}_N(\boldsymbol{\mu}) = (v_{N\,1}(\boldsymbol{\mu}), \dots, v_{N\,2N}(\boldsymbol{\mu}))^T \in \mathbb{R}^{2N}$ and $\underline{\mathbf{p}}_N(\boldsymbol{\mu}) = (p_{N\,1}(\boldsymbol{\mu}), \dots, p_{N\,N}(\boldsymbol{\mu}))^T \in \mathbb{R}^N$ are obtained by solving the following RB system:

$$\begin{bmatrix} \mathbb{A}_N(\boldsymbol{\mu}) + \mathbb{D}_N(\boldsymbol{\mu}) + \mathbb{C}_N(\underline{\mathbf{v}}_N(\boldsymbol{\mu});\boldsymbol{\mu}) & \mathbb{B}_N^T(\boldsymbol{\mu}) \\ \mathbb{B}_N(\boldsymbol{\mu}) & 0 \end{bmatrix} \begin{bmatrix} \underline{\mathbf{v}}_N(\boldsymbol{\mu}) \\ \underline{\mathbf{p}}_N(\boldsymbol{\mu}) \end{bmatrix} = \begin{bmatrix} \mathbf{f}_N(\boldsymbol{\mu}) \\ \mathbf{g}_N(\boldsymbol{\mu}) \end{bmatrix}. \tag{5.7}$$

Matrices and vectors appearing in (5.7) are defined as follows: for $1 \leq m, n \leq 2N$ and $1 \leq l \leq N$,

$$\begin{aligned} (\mathbb{A}_N(\boldsymbol{\mu}))_{mn} &= a\left(\boldsymbol{\zeta}_n^{\mathbf{v}}, \boldsymbol{\zeta}_m^{\mathbf{v}};\boldsymbol{\mu}\right), \quad (\mathbb{B}_N(\boldsymbol{\mu}))_{lm} = b\left(\zeta_l^p, \boldsymbol{\zeta}_m^{\mathbf{v}};\boldsymbol{\mu}\right), \\ (\mathbb{C}_N\left(\underline{\mathbf{w}}_N;\boldsymbol{\mu}\right))_{mn} &= \sum_{s=1}^{2N} w_{N\,s}\, c\left(\boldsymbol{\zeta}_s^{\mathbf{v}}, \boldsymbol{\zeta}_n^{\mathbf{v}}, \boldsymbol{\zeta}_m^{\mathbf{v}};\boldsymbol{\mu}\right), \\ (\mathbb{D}_N(\boldsymbol{\mu}))_{mn} &= d\left(\boldsymbol{\zeta}_n^{\mathbf{v}}, \boldsymbol{\zeta}_m^{\mathbf{v}};\boldsymbol{\mu}\right), \qquad (\mathbf{g}_N(\boldsymbol{\mu}))_l = -b\left(\zeta_l^p, \mathbf{v}_D^{\mathcal{N}};\boldsymbol{\mu}\right), \\ (\mathbf{f}_N(\boldsymbol{\mu}))_m &= F_s\left(\boldsymbol{\zeta}_m^{\mathbf{v}};\boldsymbol{\mu}\right) - a\left(\mathbf{v}_D^{\mathcal{N}}, \boldsymbol{\zeta}_m^{\mathbf{v}};\boldsymbol{\mu}\right) - c\left(\mathbf{v}_D^{\mathcal{N}}, \mathbf{v}_D^{\mathcal{N}}, \boldsymbol{\zeta}_m^{\mathbf{v}};\boldsymbol{\mu}\right). \end{aligned}$$

As before, problem (5.7) is solved by means of a *fixed-point iteration*, like in the FE case. However, with respect to (4.12), we now deal with a matrix of considerably smaller dimension ($3N \ll \mathcal{N}_V + \mathcal{N}_Q$), but no longer sparse.

[4] We should denote by $V_N^{\boldsymbol{\mu}}$ the velocity space, because of the $\boldsymbol{\mu}$-dependence of the supremizer operator. However, for the sake of simplicity, the simplest notation V^N has been preferred.

Thus, starting from the RB Stokes solution $(\underline{\mathbf{v}}_N^{(0)}(\boldsymbol{\mu}), \underline{\mathbf{p}}_N^{(0)}(\boldsymbol{\mu}))$, for $k \geq 1$, we compute $(\underline{\mathbf{v}}_N^{(k)}(\boldsymbol{\mu}), \underline{\mathbf{p}}_N^{(k)}(\boldsymbol{\mu}))$ by solving

$$\begin{bmatrix} \mathbb{A}_N(\boldsymbol{\mu}) + \mathbb{D}_N(\boldsymbol{\mu}) + \mathbb{C}_N(\underline{\mathbf{v}}_N^{(k-1)}(\boldsymbol{\mu}); \boldsymbol{\mu}) & \mathbb{B}_N^T(\boldsymbol{\mu}) \\ \mathbb{B}_N(\boldsymbol{\mu}) & 0 \end{bmatrix} \begin{bmatrix} \underline{\mathbf{v}}_N^{(k)}(\boldsymbol{\mu}) \\ \underline{\mathbf{p}}_N^{(k)}(\boldsymbol{\mu}) \end{bmatrix} = \begin{bmatrix} \mathbf{f}_N(\boldsymbol{\mu}) \\ \mathbf{g}_N(\boldsymbol{\mu}) \end{bmatrix}, \tag{5.8}$$

until $\|\mathbf{v}_N^{(k)}(\boldsymbol{\mu}) - \mathbf{v}_N^{(k-1)}(\boldsymbol{\mu})\|_V \leq \varepsilon_{\text{tol}}^{NS}$. We point out that the linearized term can be computed as

$$\sum_{n=1}^{2N} \left(\mathbb{C}_N \left(\underline{\mathbf{v}}_N^{(k-1)}(\boldsymbol{\mu}); \boldsymbol{\mu} \right) \right)_{mn} v_{N\,n}^{(k)} = \sum_{s=1}^{2N} \sum_{n=1}^{2N} v_{N\,s}^{(k-1)} c\left(\boldsymbol{\zeta}_s^{\mathbf{v}}, \boldsymbol{\zeta}_n^{\mathbf{v}}, \boldsymbol{\zeta}_m^{\mathbf{v}}; \boldsymbol{\mu}\right) v_{N\,n}^{(k)}, \quad 1 \leq m \leq 2N$$

and thus only the matrices $\mathbb{C}_N(\underline{\boldsymbol{\zeta}}_s^{\mathbf{v}}; \boldsymbol{\mu})$, for $1 \leq s \leq 2N$, $1 \leq N \leq N_{\max}$, defined by

$$\left(\mathbb{C}_N \left(\underline{\boldsymbol{\zeta}}_s^{\mathbf{v}}; \boldsymbol{\mu} \right) \right)_{mn} = c\left(\boldsymbol{\zeta}_s^{\mathbf{v}}, \boldsymbol{\zeta}_n^{\mathbf{v}}, \boldsymbol{\zeta}_m^{\mathbf{v}}; \boldsymbol{\mu}\right),$$

have to be stored. In view of an Offline/Online decomposition, it shall prove convenient to express the RB matrices and vectors appearing in (5.8) in terms of the corresponding FE matrices and vectors of (4.15). The former are linked to the latter via the basis matrices $\tilde{\mathbb{V}}_N \in \mathbb{R}^{\mathcal{N}_V \times 2N}$ and $\tilde{\mathbb{Q}}_N \in \mathbb{R}^{\mathcal{N}_Q \times N}$ given by

$$\left(\tilde{\mathbb{Q}}_N\right)_{il} = (\zeta_l^p, \phi_i^p)_Q, \quad \left(\tilde{\mathbb{V}}_N\right)_{jm} = \left(\boldsymbol{\zeta}_m^{\mathbf{v}}, \boldsymbol{\phi}_j^{\mathbf{v}}\right)_V$$

for $1 \leq i \leq \mathcal{N}_Q$, $1 \leq j \leq \mathcal{N}_V$, $1 \leq l \leq N$, $1 \leq m \leq 2N$, where (for the sake of simplicity) we denote by $(\cdot,\cdot)_Q$ and $(\cdot,\cdot)_V$ also the discrete version of the corresponding inner products defined in (2.9). We remark that the reduced bases $\{\zeta_l^p\}_{l=1}^N$, $\{\boldsymbol{\zeta}_m^{\mathbf{v}}\}_{m=1}^{2N}$, unlike the FE Lagrangian bases $\{\phi_i^p\}_{i=1}^{\mathcal{N}_Q}$ and $\{\boldsymbol{\phi}_j^{\mathbf{v}}\}_{j=1}^{\mathcal{N}_V}$, are orthonormal with respect to $(\cdot,\cdot)_Q$ and $(\cdot,\cdot)_V$, so that

$$(\zeta_l^p, \zeta_m^p)_Q = \sum_{r=1}^{\mathcal{N}_Q} \sum_{s=1}^{\mathcal{N}_Q} \left(\tilde{\mathbb{Q}}_N\right)_{ms} (\mathbb{M}_Q)_{sr} \left(\tilde{\mathbb{Q}}_N\right)_{rl} = \delta_{lm}, \qquad (\boldsymbol{\zeta}_l^{\mathbf{v}}, \boldsymbol{\zeta}_m^{\mathbf{v}})_V = \sum_{r=1}^{\mathcal{N}_V} \sum_{s=1}^{\mathcal{N}_V} \left(\tilde{\mathbb{V}}_N\right)_{ms} (\mathbb{M}_V)_{sr} \left(\tilde{\mathbb{V}}_N\right)_{rl} = \delta_{lm},$$

where $\mathbb{M}_Q \in \mathbb{R}^{\mathcal{N}_Q \times \mathcal{N}_Q}$ and $\mathbb{M}_V \in \mathbb{R}^{\mathcal{N}_V \times \mathcal{N}_V}$ are the mass matrices of $Q^{\mathcal{N}}$ and $V^{\mathcal{N}}$, whose elements are defined by $(\mathbb{M}_Q)_{sr} = (\phi_r^p, \phi_s^p)_Q$ and $(\mathbb{M}_V)_{sr} = (\boldsymbol{\phi}_r^{\mathbf{v}}, \boldsymbol{\phi}_s^{\mathbf{v}})_V$, respectively. Thus, by defining $\mathbb{Q}_N = \mathbb{M}_Q^{1/2} \tilde{\mathbb{Q}}_N$ and $\mathbb{V}_N = \mathbb{M}_V^{1/2} \tilde{\mathbb{V}}_N$, RB structures can be defined in terms of the corresponding FE structures as:

$$\mathbb{A}_N(\boldsymbol{\mu}) = \mathbb{V}_N^T\, \mathbb{A}_{\mathcal{N}}(\boldsymbol{\mu})\, \mathbb{V}_N, \qquad \mathbb{B}_N(\boldsymbol{\mu}) = \mathbb{Q}_N^T\, \mathbb{B}_{\mathcal{N}}(\boldsymbol{\mu})\, \mathbb{V}_N, \qquad \mathbb{C}_N(\underline{\boldsymbol{\zeta}}_s^{\mathbf{v}}; \boldsymbol{\mu}) = \mathbb{V}_N^T \mathbb{C}_{\mathcal{N}}(\underline{\boldsymbol{\zeta}}_s^{\mathbf{v}}; \boldsymbol{\mu}) \mathbb{V}_N, \tag{5.9}$$

for $1 \leq m, n \leq 2N$, $1 \leq l \leq N$, $1 \leq s \leq 2N$. In the same way:

$$\mathbb{D}_N(\boldsymbol{\mu}) = \mathbb{V}_N^T\, \mathbb{D}_{\mathcal{N}}(\boldsymbol{\mu})\, \mathbb{V}_N, \qquad \mathbf{f}_N(\boldsymbol{\mu}) = \mathbb{V}_N^T\, \mathbf{f}_{\mathcal{N}}(\boldsymbol{\mu}), \qquad \mathbf{g}_N(\boldsymbol{\mu}) = \mathbb{Q}_N^T\, \mathbf{g}_{\mathcal{N}}(\boldsymbol{\mu}). \tag{5.10}$$

A suitable Offline/Online decomposition strategy thus enables to decouple the generation and projection stages of the RB approximation; although quite standard in the RB context, it features some extra difficulties if nonlinear terms need to be handled in an efficient way; see Appendix A.1 for further details.

6. *A posteriori* error estimates based on BRR theory

We now derive an *a posteriori* error estimate for (affinely and nonaffinely[5]) parametrized Navier–Stokes equations in the RB context, accounting for both physical and geometrical parametrizations. Based on the BRR

[5] A first extension to nonaffinely parametrized nonlinear problems has been presented in [6] for the case of convection-diffusion problems.

theory [4, 5], this error estimate combines the dual norm of residuals and a lower bound of the (parametric) stability factor, given by the Babuška inf-sup constant $\beta_{\mathcal{N}}(\boldsymbol{\mu})$ defined in (4.10). In particular, we extend the framework already used in [7, 31] in order to deal with an Offline-Online evaluation of both these quantities.

Concerning the dual norms of residuals, their efficient evaluation is made possible thanks to the affine decomposition of Section 3.2, following a rather standard procedure in the RB context (see *e.g.* [24, 27] and [17]). However, this strategy may entail very expensive Offline precalculations and storing when dealing with nonlinear terms, in the case of large affine expansions, such as the ones obtained through EIM. Regarding the stability factors, we take advantage of a suitable extension of the natural norm SCM [18], briefly sketched in Section 7.

Let us define the residuals $r_N^{\mathbf{v}}(\cdot\,;\boldsymbol{\mu})$ and $r_N^{p}(\cdot\,;\boldsymbol{\mu})$, for any $\mathbf{w} \in V^{\mathcal{N}}$, $q \in Q^{\mathcal{N}}$, by

$$
\begin{aligned}
r_N^{\mathbf{v}}(\mathbf{w};\boldsymbol{\mu}) &:= F(\mathbf{w};\boldsymbol{\mu}) - \tilde{a}(\mathbf{v}_N(\boldsymbol{\mu}),\mathbf{w};\boldsymbol{\mu}) - b(p_N(\boldsymbol{\mu}),\mathbf{w};\boldsymbol{\mu}) - c(\mathbf{v}_N(\boldsymbol{\mu}),\mathbf{v}_N(\boldsymbol{\mu}),\mathbf{w};\boldsymbol{\mu}),\\
r_N^{p}(q;\boldsymbol{\mu}) &:= G(q;\boldsymbol{\mu}) - b(q,\mathbf{v}_N(\boldsymbol{\mu});\boldsymbol{\mu}).
\end{aligned}
$$

Equivalently, $r_N(W;\boldsymbol{\mu}) := r_N^{\mathbf{v}}(\mathbf{w};\boldsymbol{\mu}) + r_N^{p}(q;\boldsymbol{\mu})$ is such that

$$
r_N(W;\boldsymbol{\mu}) = \tilde{F}(W;\boldsymbol{\mu}) - \tilde{A}(Y_N(\boldsymbol{\mu}),W;\boldsymbol{\mu}) \qquad \forall\, W \in X^{\mathcal{N}}. \tag{6.1}
$$

Moreover, let us denote by $\|r_N(\cdot;\boldsymbol{\mu})\|_{X'} = \sup_{W\in Y^{\mathcal{N}}} r_N(W;\boldsymbol{\mu})/\|W\|_X$ the dual norm of the residual and by $\beta_{\mathcal{N}}^{\mathrm{LB}}(\boldsymbol{\mu})$ a computable lower bound for the stability factor $\beta_{\mathcal{N}}(\boldsymbol{\mu})$. We next introduce a *non-dimensional* measure of the residual, defined as:

$$
\tau_N(\boldsymbol{\mu}) = \frac{4\gamma(\rho_{\mathcal{N}};\boldsymbol{\mu})\|r_N(\cdot;\boldsymbol{\mu})\|_{X'}}{(\beta_{\mathcal{N}}^{\mathrm{LB}}(\boldsymbol{\mu}))^2}, \tag{6.2}
$$

where $\gamma(\rho_{\mathcal{N}};\boldsymbol{\mu}) \equiv \gamma_c^{\mathcal{N}}(\boldsymbol{\mu})$ is the (discrete) continuity constant of $c(\cdot,\cdot,\cdot;\boldsymbol{\mu})$, depending on the Sobolev embedding constant $\rho_{\mathcal{N}}$ defined in (4.3). We point out that (6.2) is similar to the left-hand side of (4.8) – as we will see, the condition $\tau_N(\boldsymbol{\mu}) < 1$ is strictly related to the uniqueness of the RB approximation. In particular, we can define $N^*(\boldsymbol{\mu})$ such that $\tau_N(\boldsymbol{\mu}) < 1$ for $N \geq N^*(\boldsymbol{\mu})$ and require that $N^*(\boldsymbol{\mu}) \leq N_{\max}$, for any $\boldsymbol{\mu} \in \mathcal{D}$. Furthermore, given $\overline{Y} \in X$ and $r \in \mathbb{R}_+$, we denote by $\mathcal{B}_X(\overline{Y};r) = \{Y \in X \,:\, \|Y - \overline{Y}\|_X \leq r\}$.

We are now ready to state the following

Theorem 6.1. *Let us denote by $Y^{\mathcal{N}}(\boldsymbol{\mu})$ and by $Y_N(\boldsymbol{\mu})$ the truth approximation (4.2) and the reduced basis approximation (5.2), respectively. If $N \geq N^*(\boldsymbol{\mu})$, there exists a unique solution $Y^{\mathcal{N}}(\boldsymbol{\mu})$ to (4.2) in the open ball*

$$
\mathcal{B}_X\left(Y_N(\boldsymbol{\mu}); \frac{\beta_{\mathcal{N}}^{LB}(\boldsymbol{\mu})}{2\gamma(\rho_{\mathcal{N}};\boldsymbol{\mu})}\right) = \left\{Y \in X \,:\, \|Y - Y_N(\boldsymbol{\mu})\|_X \leq \frac{\beta_{\mathcal{N}}^{LB}(\boldsymbol{\mu})}{2\gamma(\rho_{\mathcal{N}};\boldsymbol{\mu})}\right\}.
$$

Furthermore, the following a posteriori *error estimation holds:*

$$
\|Y^{\mathcal{N}}(\boldsymbol{\mu}) - Y_N(\boldsymbol{\mu})\|_X \leq \frac{\beta_{\mathcal{N}}^{LB}(\boldsymbol{\mu})}{2\gamma(\rho_{\mathcal{N}};\boldsymbol{\mu})}\left(1 - \sqrt{1 - \tau_N(\boldsymbol{\mu})}\right) =: \Delta_N(\boldsymbol{\mu}) \quad \forall\, \boldsymbol{\mu} \in \mathcal{D}. \tag{6.3}
$$

Proof. The result can be obtained as a slight variation of Proposition 2.1 of [31], by considering the operator $g(W,V;\boldsymbol{\mu}) = \tilde{A}(W,V;\boldsymbol{\mu}) - \tilde{F}(V;\boldsymbol{\mu})$, and remarking that $\mathrm{d}g(Z;W,V;\boldsymbol{\mu}) = \mathrm{d}\tilde{A}(Z;W,V;\boldsymbol{\mu})$. It essentially follows the proof of the *inverse function theorem* (see *e.g.* Thm. 2.1 of [5]); further details can be found in [17]. □

In this way, we can generalize the available *a posteriori* error bounds for NS equations as follows: (i) by considering the global NS operator $\tilde{A}(\cdot,\cdot;\boldsymbol{\mu})$ (including also the pressure terms) and the lower bound $\beta_{\mathcal{N}}^{\mathrm{LB}}(\boldsymbol{\mu})$, we provide a joint error estimate for both RB velocity and pressure; (ii) by considering the continuity factor $\gamma(\rho_{\mathcal{N}};\boldsymbol{\mu})$ of the trilinear form instead of the Sobolev embedding constant $\rho_{\mathcal{N}}$ such as, *e.g.*, in [31], we can deal with problems involving parametrized trilinear terms – obtained, for instance, when dealing with parametrized geometries. Moreover, in the case of nonaffine problems the correction factor $\max_{q=1,\ldots,Q_c} \|\eta^q\|_{L^\infty(\Omega)}$ affects the definition of $\gamma(\rho_{\mathcal{N}};\boldsymbol{\mu})$, whereas it reduces to 1 in the affine case – see (3.5).

Remark 6.2. Note that (6.3) can be seen as the nonlinear extension of the – much simpler – Stokes (linear) error bound $\Delta_{N,s}(\boldsymbol{\mu}) = \|r_N(\boldsymbol{\mu})\|_{X'}/\beta^{\mathrm{LB}}_{A,\mathcal{N}}(\boldsymbol{\mu})$ (for both velocity and pressure), being $\beta^{\mathrm{LB}}_{A,\mathcal{N}}(\boldsymbol{\mu})$ a lower bound of the stability factor of the Stokes operator (see e.g [26], Sect. 6), to which (6.3) reduces in the limit $\|r_N(\cdot;\boldsymbol{\mu})\|_{X'} \to 0$.

Very often, the efficient evaluation of stability factors of parametrized operators is the most challenging stage of the whole procedure. To this aim, we have developed in [18] a SCM algorithm which can be performed before (and independently from) the generation of a reduced approximation. This strategy relies on a simple *trick* motivated by the continuity of the trilinear form $c(\cdot,\cdot,\cdot;\boldsymbol{\mu})$. In fact, since the error bound is related to the RB solution $Y_N(\boldsymbol{\mu})$, the derivative of the global operator and the stability factor have to be evaluated with respect to $Y_N(\boldsymbol{\mu})$. Thus, we should replace $Y^{\mathcal{N}}(\boldsymbol{\mu})$ with $Y_N(\boldsymbol{\mu})$ and consider

$$\beta^N_{\mathcal{N}}(\boldsymbol{\mu}) = \inf_{U\in X^{\mathcal{N}}} \sup_{W\in X^{\mathcal{N}}} \frac{\mathrm{d}\tilde{A}(Y_N(\boldsymbol{\mu});\boldsymbol{\mu})(U,W)}{\|U\|_X\|W\|_X} \tag{6.4}$$

instead of (4.10). However, evaluating (6.4) would be infeasible during the Offline stage, if we aim at evaluating the lower bound of the stability factor *before* running the greedy algorithm for the construction of the RB space. Thus, we compute a lower bound to $\beta_{\mathcal{N}}(\boldsymbol{\mu})$ defined by (4.10), instead of $\beta^N_{\mathcal{N}}(\boldsymbol{\mu})$, because we have that

$$\left|\beta_{\mathcal{N}}(\boldsymbol{\mu}) - \beta^N_{\mathcal{N}}(\boldsymbol{\mu})\right| \le 2\gamma^{\mathcal{N}}_c(\boldsymbol{\mu}) \left\|Y^{\mathcal{N}}(\boldsymbol{\mu}) - Y_N(\boldsymbol{\mu})\right\|_X \qquad \forall \boldsymbol{\mu}\in\mathcal{D},$$

by exploiting the trilinearity and the continuity of $c(\cdot,\cdot;\boldsymbol{\mu})$. Provided the error $\|Y^{\mathcal{N}}(\boldsymbol{\mu}) - Y_N(\boldsymbol{\mu})\|_X$ is sufficiently small, $\beta_{\mathcal{N}}(\boldsymbol{\mu})$ yields a very accurate approximation of $\beta^N_{\mathcal{N}}(\boldsymbol{\mu})$, giving the chance to estimate a lower bound to the (discrete) stability factor $\beta_{\mathcal{N}}(\boldsymbol{\mu})$ – indeed very close to $\beta^N_{\mathcal{N}}(\boldsymbol{\mu})$ – before assembling the reduced space. Results reported in [18] confirm the accuracy of this approximation: as a matter of fact, we get an estimate $2\gamma^{\mathcal{N}}_c(\boldsymbol{\mu})\|Y^{\mathcal{N}}(\boldsymbol{\mu}) - Y_N(\boldsymbol{\mu})\|_X$ of order 10^{-4} and an effective error $|\beta_{\mathcal{N}}(\boldsymbol{\mu}) - \beta^N_{\mathcal{N}}(\boldsymbol{\mu})|$ of order 10^{-5}, when $N = N_{\max}$, together with a very fast decay with respect to N. In any case, a good error control can be ensured by choosing a suitable stopping tolerance in the greedy procedure.

7. Approximation of lower bounds of stability factors

In this section we sketch the main ingredients of a recent extension of the SCM to the case of nonlinear parametrized operators, presented in [18]. Based on the successive solution of suitable linear optimization problems, SCM has been developed for the special requirements of the RB method, such as an efficient Offline-Online strategy. A general version using the so-called *natural norm* has been introduced in [29] and further analyzed in [13]; furthermore, it has been applied for the first time to saddle point Stokes problems in [26]. Very recently, we have provided some theoretical justifications allowing to extend this method to nonlinear problems in an efficient way, as discussed in the previous section. We have taken advantage of this extension in the present RB framework for NS equations, in order to estimate a lower bound of the stability factor $\beta_{\mathcal{N}}(\boldsymbol{\mu})$.

To reach this goal, we can rewrite $\beta_{\mathcal{N}}(\boldsymbol{\mu})$ as

$$\beta_{\mathcal{N}}(\boldsymbol{\mu}) := \inf_{U\in X^{\mathcal{N}}} \sup_{W\in X^{\mathcal{N}}} \frac{\mathrm{d}\tilde{A}\left(Y^{\mathcal{N}};\boldsymbol{\mu}\right)(U,W)}{\|U\|_X\|W\|_X} = \inf_{U\in X^{\mathcal{N}}} \frac{\mathrm{d}\tilde{A}\left(Y^{\mathcal{N}};\boldsymbol{\mu}\right)(U,T^{\boldsymbol{\mu}}U;\boldsymbol{\mu})}{\|U\|_X\|T^{\boldsymbol{\mu}}U\|_X} \tag{7.1}$$

by introducing the (global) supremizer operator $T^{\boldsymbol{\mu}} : X^{\mathcal{N}} \to X^{\mathcal{N}}$, defined as

$$(T^{\boldsymbol{\mu}}U, W)_X = \mathrm{d}\tilde{A}\left(Y^{\mathcal{N}};\boldsymbol{\mu}\right)(U,W) \quad \forall\, W\in X^{\mathcal{N}}, \tag{7.2}$$

such that, similarly to (4.7)

$$T^{\boldsymbol{\mu}}U = \arg\sup_{W\in X^{\mathcal{N}}} \frac{\mathrm{d}\tilde{A}(Y^{\mathcal{N}};\boldsymbol{\mu})(U,W)}{\|W\|_X} \quad \text{and} \quad (\beta_{\mathcal{N}}(\boldsymbol{\mu}))^2 = \inf_{U\in X^{\mathcal{N}}} \frac{\|T^{\boldsymbol{\mu}}U\|^2_X}{\|U\|^2_X}. \tag{7.3}$$

Following [13, 29], we adopt a *natural norm* SCM procedure based on the patching of some local inf-sup stability factors computed for a set of J parameter values $\mathcal{S} = \{\boldsymbol{\mu}^{1*}, \dots, \boldsymbol{\mu}^{J*}\}$, selected *e.g.* through a greedy procedure; detailed proofs and computational procedures can be found in [18].

The key observation is provided by the following relation:

$$\begin{aligned}\beta_{\mathcal{N}}(\boldsymbol{\mu}) &= \inf_{U\in X^{\mathcal{N}}} \sup_{W\in X^{\mathcal{N}}} \frac{\mathrm{d}\tilde{A}\left(Y^{\mathcal{N}}(\boldsymbol{\mu});\boldsymbol{\mu}\right)(U,W)}{\|T^{\mu^*}W\|_X\|U\|_X}\frac{\|T^{\mu^*}W\|_X}{\|W\|_X} \\ &\geq \inf_{U\in X^{\mathcal{N}}} \sup_{W\in X^{\mathcal{N}}} \frac{\mathrm{d}A\left(Y^{\mathcal{N}}(\boldsymbol{\mu});\boldsymbol{\mu}\right)(U,W)}{\|T^{\mu^*}W\|_X\|U\|_X} \inf_{W\in X^{\mathcal{N}}} \frac{\|T^{\mu^*}W\|_X}{\|W\|_X} = \beta_{\boldsymbol{\mu}^*}(\boldsymbol{\mu})\beta_{\mathcal{N}}(\boldsymbol{\mu}^*) \geq \tilde{\beta}_{\boldsymbol{\mu}^*}(\boldsymbol{\mu})\beta_{\mathcal{N}}\left(\boldsymbol{\mu}^*\right). \end{aligned} \tag{7.4}$$

Here $\beta_{\boldsymbol{\mu}^*}(\boldsymbol{\mu})$ is a *surrogate* of $\beta_{\mathcal{N}}(\boldsymbol{\mu})$ upon $\boldsymbol{\mu}^* \in \mathcal{S}$, whereas $\tilde{\beta}_{\boldsymbol{\mu}^*}(\boldsymbol{\mu})$ is a lower bound such that

$$\begin{aligned}\tilde{\beta}_{\boldsymbol{\mu}^*}(\boldsymbol{\mu}) &:= \inf_{U\in X^{\mathcal{N}}} \frac{\mathrm{d}\tilde{A}(Y^{\mathcal{N}}(\boldsymbol{\mu});\boldsymbol{\mu})(U,T^{\mu^*}U)}{\|T^{\mu^*}U\|_X^2} \\ &\leq \inf_{U\in X^{\mathcal{N}}} \frac{\|T^{\boldsymbol{\mu}}U\|_X}{\|T^{\mu^*}U\|_X} = \inf_{U\in X^{\mathcal{N}}} \sup_{W\in Y^{\mathcal{N}}} \frac{\mathrm{d}\tilde{A}(Y^{\mathcal{N}}(\boldsymbol{\mu});\boldsymbol{\mu})(U,W)}{\|T^{\mu^*}U\|_X\|W\|_X} =: \beta_{\boldsymbol{\mu}^*}(\boldsymbol{\mu}), \end{aligned} \tag{7.5}$$

thanks to Cauchy–Schwarz inequality and the fact that $\mathrm{d}\tilde{A}(Y^{\mathcal{N}};\boldsymbol{\mu})(W,T^{\mu^*}W) = (T^{\boldsymbol{\mu}}W,T^{\mu^*}W)$. We call $\|T^{\mu^*}\cdot\|_X$ the *natural norm*; it is equivalent to $\|\cdot\|_X$ in a neighborhood $\mathcal{P}_{\boldsymbol{\mu}^*} \ni \boldsymbol{\mu}^*$ since we assume that $\beta_{\mathcal{N}}(\boldsymbol{\mu}) > 0\ \forall \boldsymbol{\mu} \in \mathcal{D}$.

Concerning the evaluation of $\tilde{\beta}_{\boldsymbol{\mu}^*}(\boldsymbol{\mu})$, the key point is the possibility to define this quantity as the solution of a *linear program* of dimension $Q_a + Q_b + Q_c$. Thus, an approximated lower bound of $\tilde{\beta}_{\boldsymbol{\mu}^*}(\boldsymbol{\mu})$ results from the solution of a sequence of suitable relaxed linear programs, obtained by adding iteratively a set of constraints. See *e.g.* [13,18] for a detailed explanation of such a procedure. We only remark that the (Offline) solution of the linear programs entails the evaluation of the NS solution $Y^{\mathcal{N}}(\boldsymbol{\mu}^*)$ for $\boldsymbol{\mu} = \boldsymbol{\mu}^*$ and for any $\boldsymbol{\mu} = \hat{\boldsymbol{\mu}}_*$ corresponding to a new added constraint. Moreover, this strategy is suitable for an efficient Offline/Online evaluation of the lower bound, for any new $\boldsymbol{\mu} \in \mathcal{D}$, which clearly does not require to obtain $Y^{\mathcal{N}}(\boldsymbol{\mu})$.

Remark 7.1. Using the natural norm $\|T^{\boldsymbol{\mu}}\cdot\|_X$ to equip the space $X = V \times Q$ instead of (2.9), would lead to more effective bounds, as shown *e.g.* in [7]. However, since this norm is $\boldsymbol{\mu}$-dependent, it is computationally expensive in the case of $p \geq 2$ parameters and/or large affine expansions of the parametrized operators; for this reason we have decided to use the natural norm just during the SCM algorithm. In this way, the SCM stage is decoupled from the greedy algorithm for the assembling of the RB space; as a matter of fact, also bases orthonormalization and Sobolev embedding constants evaluation are less involved. Furthermore, by equipping Q with a weighted L^2 norm, and using a natural norm in the SCM algorithm, we obtain larger lower bounds $\beta_{\mathcal{N}}^{\mathrm{LB}}(\boldsymbol{\mu})$, thus improving the effectivity of the error estimate (6.3).

We refer to [18] for a detailed explanation of the SCM algorithm in the NS case; we only point out that, in this latter case, further (expensive) calculations are required with respect to the Stokes case, due to the (linearization of) nonlinear operators and the solution of a high-fidelity NS problem for each selected $\boldsymbol{\mu}^{j*}$, as well as for each added constraint [13]. This features a large additional cost, since the SCM algorithm may take several iterations to converge. For this reason, we have taken into account some heuristic (but cheaper) alternatives to deal with the case of $p > 2$ parameters. For instance, we can consider the approximation of a global lower bound by seeking for the minimum of $\beta_{\mathcal{N}}(\boldsymbol{\mu})$ all over the parameter space $\mathcal{D}$ through a numerical optimization procedure. Although it provides less effective lower bounds, this alternative strategy is more feasible, provided the convergence is rapid – note that each evaluation entails the solution of both a high-fidelity NS problem and an eigenproblem for the linearized NS operator – and $\beta_{\mathcal{N}}(\boldsymbol{\mu})$ does not show strong parametric variations. This latter requirement is fulfilled, *e.g.*, when dealing with geometrical parametrizations featuring small deformations. Better options could involve, for instance, an interpolation of the function $\boldsymbol{\mu} \to \beta_{\mathcal{N}}(\boldsymbol{\mu})$ built *e.g.* with radial basis functions, which are well suited for interpolating scattered data and thus require potentially few evaluations of $\beta_{\mathcal{N}}(\boldsymbol{\mu})$. We remind the interested reader to [18] for further details.

8. Approximation of Sobolev embedding constants

We present here a fixed-point algorithm for the computation of the (discrete) Sobolev constant (4.3). This algorithm has been firstly addressed in [7]; here we provide a complete proof of the theoretical results it is built over. To set this procedure, we need to reformulate the evaluation of the Sobolev constant (4.3) as a fixed point iteration for a suitable operator involving the solution of an eigenproblem.

In this section we refer to discrete functions and spaces by omitting the dependence on $\mathcal{N}$, so that here $(v,v)_V$ denotes the inner product $(\nabla v, \nabla v)_{L^2(\Omega)}$ $\forall v \in V^{\mathcal{N}}$ (we consider the approximation $\rho_{\mathcal{N}}$ of the Sobolev constant ρ defined in (3.6)). First of all, let us denote with u_* the element of $V^{\mathcal{N}}$ (not necessarily unique) satisfying

$$u_* = \arg\max_{v \in V^{\mathcal{N}}} \frac{\|v\|_4^2}{(v,v)_V}, \qquad (u_*, u_*)_V = 1. \tag{8.1}$$

Then, let us define the operator $\sigma : V^{\mathcal{N}} \to V^{\mathcal{N}}$ as

$$\sigma(w) = w^2 / \|w\|_4^2; \tag{8.2}$$

note that $\|\sigma(w)\|_2 = 1$, for all $w \in V^{\mathcal{N}}$. Thus, given a nonnegative function $z \in L^2(\Omega)$, let us introduce the following eigenproblems: for each $1 \le i \le \mathcal{N}$, $u_i(z) \in V^{\mathcal{N}}$ and $\lambda_i(z) \in \mathbb{R}_+$ are solution of

$$\int_\Omega z u_i(z) v = \lambda_i(z)(u_i(z), v)_{V^{\mathcal{N}}} \quad \forall v \in V^{\mathcal{N}}, \quad \text{with} \quad (u_i(z), u_i(z))_V = 1. \tag{8.3}$$

Here we consider the eigenvalues $\{\lambda_i(z)\}_{i=1}^{\mathcal{N}}$ in increasing order, with $0 \le \lambda_1(z) \le \ldots \le \lambda_{\mathcal{N}}(z)$, and denote with $u_{\max}(z) = u_{\mathcal{N}}(z)$. We remark that

$$\lambda_{\max}(z) = \max_{v \in V^{\mathcal{N}}} \left(\frac{1}{(v,v)_V} \int_\Omega z v^2 \right) \tag{8.4}$$

by definition of Rayleigh quotient. A fixed-point iteration for the approximation of $\rho_{\mathcal{N}}^2$ is motivated by the following

Lemma 8.1. *The discrete Sobolev embedding constant $\rho_{\mathcal{N}}$ and the element u_* defined by (4.3) and (8.1), respectively, satisfy*

$$\lambda_{\max}(\sigma(u_*)) = \rho_{\mathcal{N}}^2, \qquad u_{\max}(\sigma(u_*)) = u_*.$$

See Appendix A.2 for the proof. Thus, in order to develop a fixed-point procedure based on the above result, we point out that, by denoting $\partial u := u_{\max}(z_2) - u_{\max}(z_1)$

$$\begin{aligned} \lambda_{\max}(z_2) - \lambda_{\max}(z_1) &= \int_\Omega z_2 u_{\max}^2(z_2) - \int_\Omega z_1 u_{\max}^2(z_1) \\ &= \int_\Omega (z_2 - z_1) u_{\max}^2(z_1) + \int_\Omega z_2 u_{\max}(z_2) \delta u + \int_\Omega z_1 u_{\max}(z_1) \delta u + \int_\Omega (z_2 - z_1) u_{\max}(z_1) \delta u. \end{aligned} \tag{8.5}$$

We can show (see Appendix A.3 for the proof) the following

Lemma 8.2. *Given two non-negative functions $z_1, z_2 \in L^2(\Omega)$, the corresponding maximum eigenvalues $\lambda_{\max}(z_1)$, $\lambda_{\max}(z_2)$ defined by (8.4) are such that*

$$\lambda_{\max}(z_2) - \lambda_{\max}(z_1) = \int_\Omega (z_2 - z_1) u_{\max}^2(z_1) + \mathcal{O}(\|z_2 - z_1\|_2^2).$$

We are now ready to set a fixed point algorithm for the evaluation of the Sobolev embedding constant. Starting from $z^{(0)} = 1$, for $k = 1, 2, \ldots$, we evaluate

$$\phi^{(k)} = \lambda_{\max}\left(z^{(k-1)}\right); \quad z^{(k)} = \sigma\left(u_{\max}\left(z^{(k-1)}\right)\right),$$

until $|\phi^{(k)} - \phi^{(k-1)}| < \varepsilon_{\text{tol}}^{\text{Sob}}$, given a prescribed tolerance $\varepsilon_{\text{tol}}^{\text{Sob}} > 0$. In order to prove that $\phi^{(k)} \to \rho_{\mathcal{N}}^2$ as $k \to \infty$, we observe that, owing to Lemma 8.2, the following relationship holds:

$$\begin{aligned}\phi^{(k+1)} - \phi^{(k)} &= \lambda_{\max}\left(z^{(k)}\right) - \lambda_{\max}\left(z^{(k-1)}\right) \\ &= \int_\Omega \left(\sigma(u_{\max}\left(z^{(k-1)}\right)\right) - \sigma\left(u_{\max}\left(z^{(k-2)}\right)\right) u_{\max}^2\left(z^{(k-1)}\right) + \mathcal{O}\left(\left\|z^{(k-1)} - z^{(k-2)}\right\|_2^2\right). \quad (8.6)\end{aligned}$$

At this point, it just remains to show that the first term in the last expression is non-negative, so that the fixed-point iteration at least heads in the right direction – we remark that a fixed point of the algorithm is not the supremizer of (8.4), but it is at least a *local* supremizer. Thanks to definition (8.2), the factor $u_{\max}^2(z^{(k-1)})$ appearing in (8.6) can be rewritten as $u_{\max}^2(z^{(k-1)}) = \sigma(u_{\max}(z^{(k-1)}))\|u_{\max}(z^{(k-1)})\|_4^2$, so that

$$\begin{aligned}&\int_\Omega \left(\sigma\left(u_{\max}\left(z^{(k-1)}\right)\right) - \sigma\left(u_{\max}\left(z^{(k-2)}\right)\right)\right) u_{\max}^2\left(z^{(k-1)}\right) \\ &\qquad = \left\|u_{\max}\left(z^{(k-1)}\right)\right\|_4^2 \left(\sigma\left(u_{\max}\left(z^{(k-1)}\right)\right), \sigma\left(u_{\max}\left(z^{(k-1)}\right)\right) - \sigma\left(u_{\max}\left(z^{(k-2)}\right)\right)\right)_2 \quad (8.7)\end{aligned}$$

is a positive quantity (see Appendix A.3 for the proof).

In particular, we observed a very fast convergence of the fixed point algorithm above. In fact, it requires no more than 10 iterations to compute the Sobolev embedding constants for the test cases presented in the following section, by choosing a tolerance $\varepsilon_{\text{tol}}^{\text{Sob}} = 10^{-5}$. In any case, evaluating the Sobolev constant is an Offline operation, since this quantity does not depend on parameters (recall that in case of geometrical parameters, computations are performed on a fixed, reference domain).

9. Numerical results

In this section we present some numerical results for moderate Reynolds viscous flows in different geometries. Proceeding by increasing complexity, we consider a flow over a backward facing step parametrized by the Reynolds number (Sect. 9.1); in a double elbow duct parametrized by the Reynolds number and the aspect ratio (Sect. 9.2); and around an airfoil profile, whose shape is parametrized through a set of control points (Sect. 9.3). All the details concerning the construction of RB spaces and the computational performances are reported in Section 9.4.

9.1. Case 1. Flow over a backward facing step

We consider a parametrized flow over a backward facing step geometry, reported in Figure 1. We denote by Ω_k, $k = 1, 2$ the portions of the channel with different sectional area, and consider $p = 1$ parameter, the Reynolds number $\mu_1 = Re \in \mathcal{D} = [10, 250]$. Here the domain is parameter-independent, thus $\tilde{\Omega}_k \equiv \Omega_k$. A parabolic flow $\mathbf{g}_D$ is imposed at the inlet $\Gamma_{D_g} = \Gamma_1$, such that $\int_{\Gamma_1} \mathbf{g}_D = 1$, while a free-stress condition ($\mathbf{g}_N = \mathbf{0}$) is imposed at the outflow $\Gamma_N = \Gamma_5$; the forcing term is $\mathbf{f} = (0, 0)$. Here we have that $Re = 1/\nu$, since both the characteristic length, *i.e.* the channel width at the inflow, and the characteristic velocity $|\bar{\mathbf{v}}| = \int_{\Gamma_1} \mathbf{g}_D$, are equal to 1.

Concerning the Offline stage, we rely on a $\mathbb{P}_2 - \mathbb{P}_1$ FE approximation, and first we run the SCM algorithm. In Figure 2 (left) we report the values of the stability factor $\beta_{\mathcal{N}}(\boldsymbol{\mu})$ together with the lower bounds $\beta_{\mathcal{N}}^{LB}(\boldsymbol{\mu})$. Note the approximation is made by $J = 7$ local patches, each of them centered around $\boldsymbol{\mu}^{1*}, \ldots, \boldsymbol{\mu}^{J*}$.

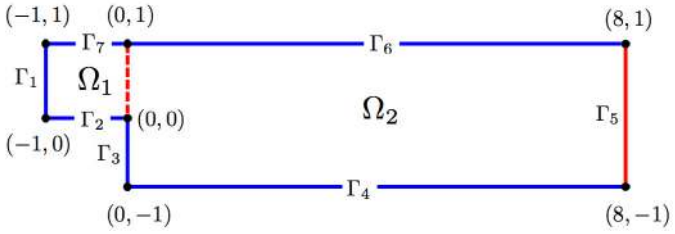

FIGURE 1. Case 1. Parametrized geometry and domain boundaries.

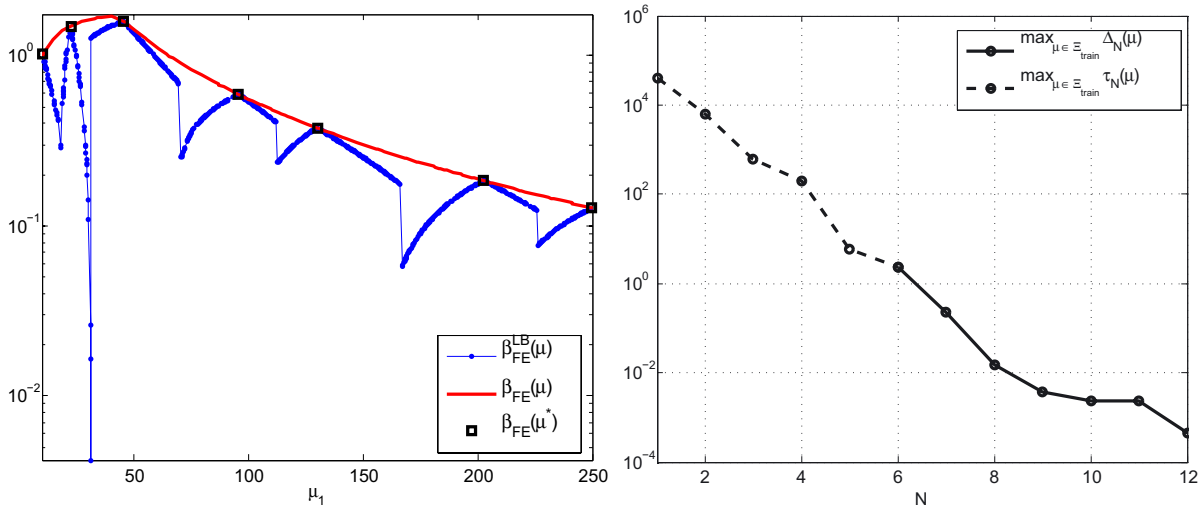

FIGURE 2. Case 1. Left: stability factor $\beta_{\mathcal{N}}(\boldsymbol{\mu})$ and lower bound $\beta_{\mathcal{N}}^{LB}(\boldsymbol{\mu})$ as functions of $\boldsymbol{\mu}$; black squares indicate the computed values $\beta_{\mathcal{N}}(\boldsymbol{\mu}^*)$ by SCM. Right: convergence of the greedy algorithm; here Ξ_{train} is a uniform random sample of size $n_{\text{train}} = 500$, $\varepsilon_{\text{tol}}^{\text{RB}} = 5 \times 10^{-3}$.

Then, we run the greedy algorithm for the construction of the RB spaces. Through this procedure, we select $N_{\max} = 12$ basis functions with a prescribed tolerance $\varepsilon_{\text{tol}}^{\text{RB}} = 5 \times 10^{-3}$. The convergence of the greedy algorithm is reported in Figure 2 (right).

Regarding the Online stage, evaluation of the errors between the FE and the RB approximations (over a train sample Ξ_{test} of size $n_{\text{test}} = 50$, for $N = 1, \ldots, N_{\max}$) and the corresponding error bounds are reported in Figure 3. In this case we have $N^*(\boldsymbol{\mu}) = 6$ (recall that $N^*(\boldsymbol{\mu})$ is such that $\tau_N(\boldsymbol{\mu}) < 1$ for $N \geq N^*(\boldsymbol{\mu})$), whereas we can keep $\tau_N(\boldsymbol{\mu})$ as error bound for $N < N^*(\boldsymbol{\mu})$. We also plot the linear error bound $\Delta_{N,s}(\boldsymbol{\mu})$, which results proportional to $\tau_N(\boldsymbol{\mu})$, and indeed very close to $\Delta_N(\boldsymbol{\mu})$ for $N \geq N^*(\boldsymbol{\mu})$. We can remark that the effectivity of the error bound, *i.e.* the ratio between the error estimate $\Delta_N(\boldsymbol{\mu})$ and the computed error, is in any case of about 10^2. We report in Figure 3 (right) the errors and the error bounds for $N = N_{\max}$, as functions of $\boldsymbol{\mu}$.

As we can see in Figure 3 (left), the (norm of) RB approximation errors decreases quite rapidly when N increases, uniformly over the parameter space. In fact, the maximum error (jointly for velocity and pressure) is of order 10^{-2} when $N = 6$, of order 10^{-4} when $N = 10$, and drops to 10^{-5} when $N = N_{\max} = 12$. Moreover, the location of the selected snapshots – *i.e.*, those parameter values belonging to $S_N = \{\boldsymbol{\mu}^1, \ldots, \boldsymbol{\mu}^N\}$ – is rather evident, thus confirming the *consistency* of the RB approximation. As a matter of fact, the Online evaluation obtained by choosing $\boldsymbol{\mu} \in S_N$ yields approximation errors which are close to working precision.

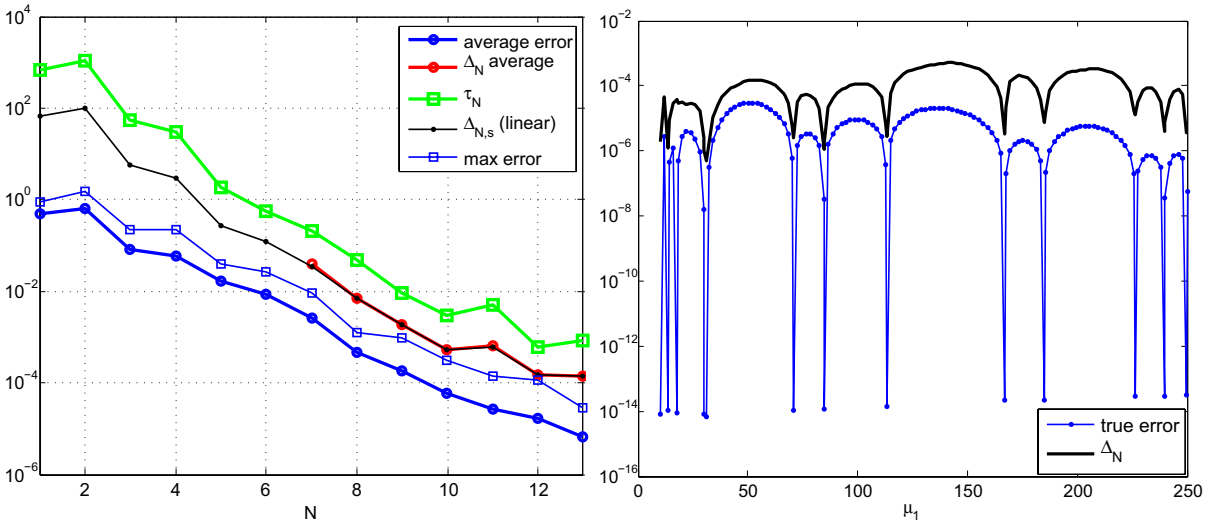

FIGURE 3. Case 1. Left: online evaluations of error bounds $\Delta_N(\boldsymbol{\mu})$ (maximum and average over $n_{\text{test}} = 50$ sampled $\boldsymbol{\mu}$ values), Stokes (linear) error bounds $\Delta_{N,s}(\boldsymbol{\mu})$ (average), indicators $\tau_N(\boldsymbol{\mu})$ (maximum) and errors (average and maximum) between FE and RB approximations. Right: online evaluations of errors and error bounds $\Delta_N(\boldsymbol{\mu})$ as functions of $\boldsymbol{\mu}$, for $N = N_{\max}$.

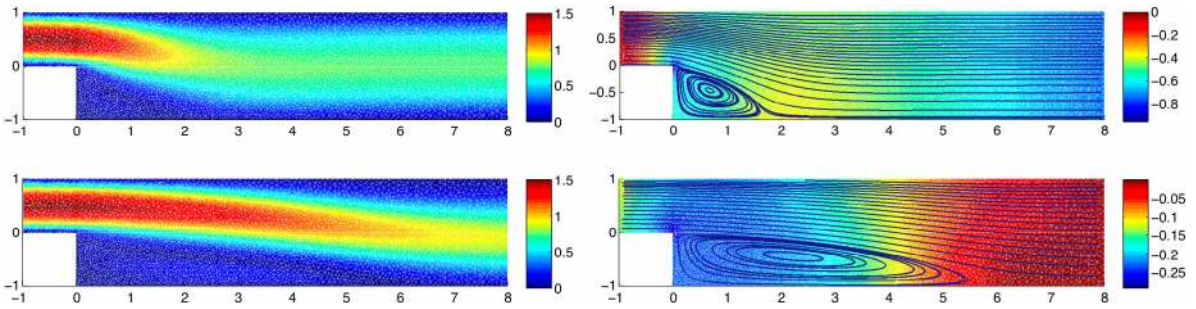

FIGURE 4. Case 1. RB solutions for velocity and pressure with streamlines for $\boldsymbol{\mu} = 50$ (top) and $\boldsymbol{\mu} = 250$ (bottom).

In Figure 4 we plot some representative solutions. The presence of a flow separation caused by the sudden change in section geometry, as well as of an increasingly larger recirculation with increasing Reynolds numbers, are recovered also by the RB approximation, as expected (see *e.g.* [2]).

Finally, we report in Figure 5 the errors between FE and RB approximations, for both the pressure and the velocity field, by considering $\boldsymbol{\mu} = 50, 150, 250$. We can remark that pointwise errors over the spatial domain are indeed very small, provided a good sampling of the parameter space has been performed during the Offline stage. In particular, errors for both velocity and pressure fields in the cases $\boldsymbol{\mu} = 50, 150$ are of order 10^{-5}, and even smaller for $\boldsymbol{\mu} = 250$, according to the behavior of the error norms reported in Figure 3 (right).

9.2. Case 2. Flow in a parametrized double elbow geometry

We now consider a parametrized flow in the geometrical configuration of Figure 6, representing a double elbow pipeline. We identify the (now parametrized) regions Ω_k, $1 \le k \le 3$, which represent the three portions of the channel with constant sizes ($k = 1, 3$) and variable sizes ($k = 2$). We consider $p = 2$ parameters, $\mu_1 = 1/\nu$ and

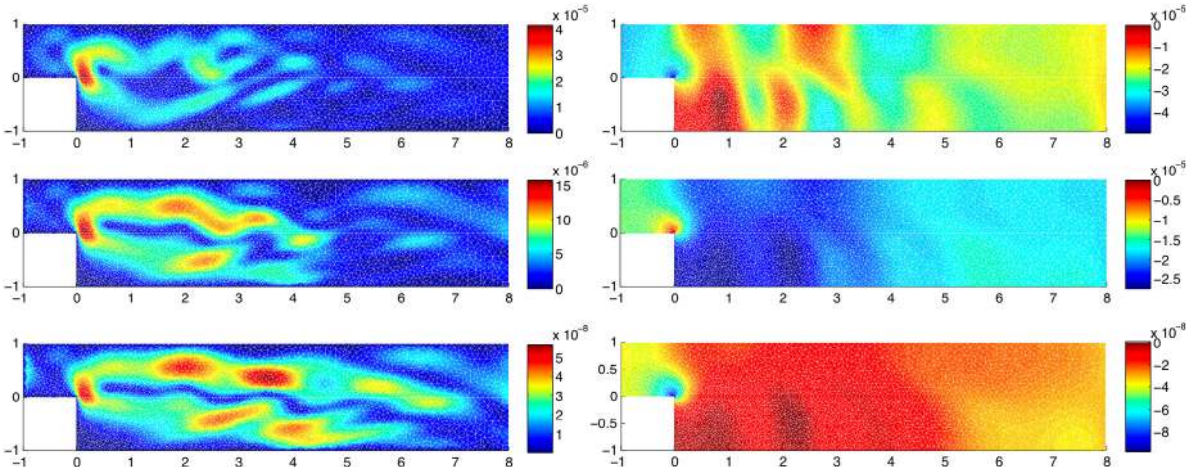

FIGURE 5. Case 1. Errors between FE and RB approximations for velocity (left) and pressure (right) for $\boldsymbol{\mu} = 50$ (top), $\boldsymbol{\mu} = 150$ (middle) and $\boldsymbol{\mu} = 250$ (bottom). The RB approximation is computed with $N = N_{\max} = 12$ basis functions.

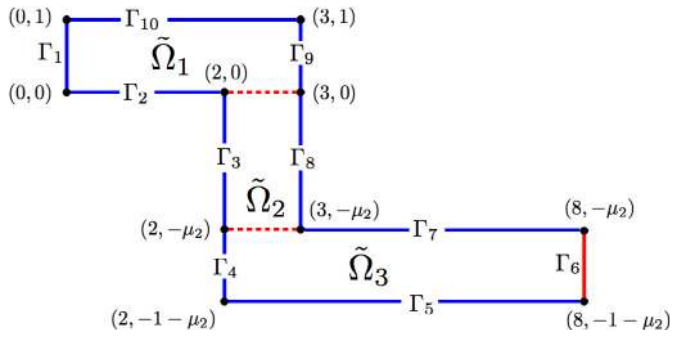

FIGURE 6. Parametrized geometry and domain boundaries for the double elbow pipeline case.

the aspect ratio μ_2 of the vertical portion of the pipeline; the parameter domain is given by $\mathcal{D} = [20, 150] \times [2, 5]$. A parabolic flow $\mathbf{g}_D$ is imposed at the inlet $\Gamma_{D_g} = \Gamma_1$, such that $\max_{\Gamma_1} \mathbf{g}_D = 1$, while a free-stress condition ($\mathbf{g}_N = \mathbf{0}$) is imposed at the outflow $\Gamma_N = \Gamma_6$ and $\mathbf{f} = (0, 0)$. Here we have $Re = \mu_1$, provided we assume as characteristic length L the channel width, and as characteristic velocity $|\bar{\mathbf{v}}| = \max_{\Gamma_1} \mathbf{g}_D$, both equal to 1.

Concerning the Offline stage, we rely on a $\mathbb{P}_2 - \mathbb{P}_1$ FE approximation, and first we run the SCM algorithm. In Figure 7 we report the values of the stability factor $\beta_{\mathcal{N}}(\boldsymbol{\mu})$ together with the lower bounds $\beta^{LB}_{\mathcal{N}}(\boldsymbol{\mu})$ obtained by the SCM algorithm. We remark that, with respect to test case 1, here the approximation of the lower bound is made by many more local patches, because of the interplay between the geometrical and the physical element, and that the $J = 176$ selected parameter values $\boldsymbol{\mu}^{1*}, \ldots, \boldsymbol{\mu}^{J*}$ are gathered close to larger values of $\mu_1 = Re$. We experienced the same behavior of the SCM algorithm in other test cases related to NS flows parametrized with respect to both physical and geometrical quantities. The rather poor rate of convergence of such a procedure occurring in this case has been one of the main reasons which have motivated the implementation of heuristic strategies, in order to evaluate stability factors in a reasonable time.

Then, we run the greedy algorithm for the construction of the RB spaces; its convergence is reported in Figure 8 (left). In this case, $N_{\max} = 30$ basis functions are selected, with a prescribed tolerance $\varepsilon^{\text{RB}}_{\text{tol}} = 5 \times 10^{-2}$.

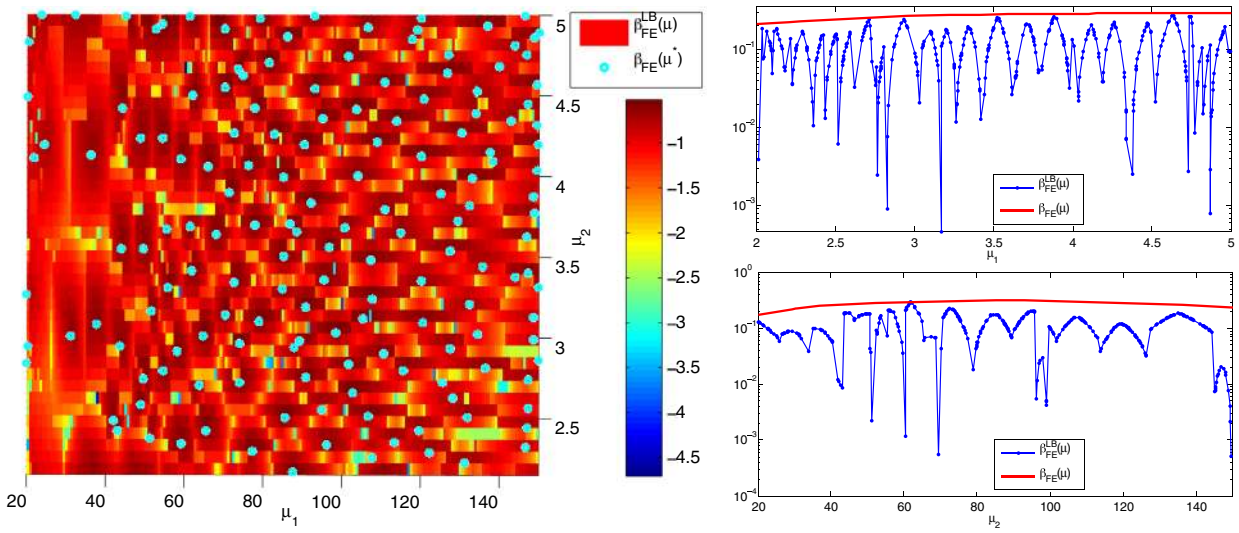

FIGURE 7. Case 2. Left: lower bound of the stability factor $\beta_{\mathcal{N}}^{LB}(\boldsymbol{\mu})$ as function of (μ_1, μ_2) and computed values $\beta_{\mathcal{N}}(\boldsymbol{\mu}^*)$ during the SCM algorithm. Right: stability factor $\beta_{\mathcal{N}}(\boldsymbol{\mu})$ and lower bound $\beta_{\mathcal{N}}^{LB}(\boldsymbol{\mu})$ for $\mu_1 = 125$ (top) and $\mu_2 = 3.25$.

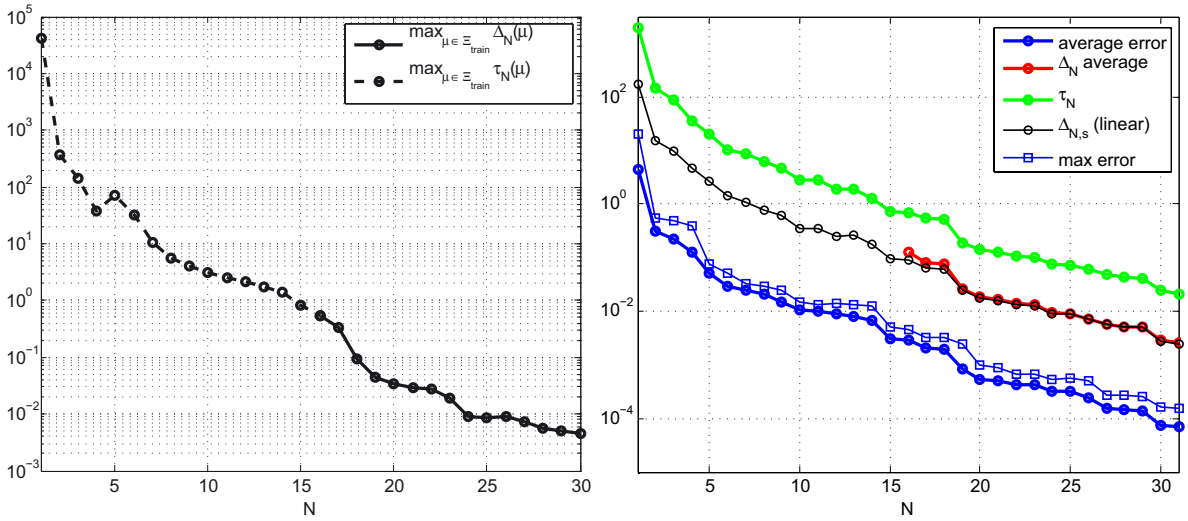

FIGURE 8. Case 2. Left: convergence of the greedy algorithm; here Ξ_{train} is a uniform random sample of size $n_{\text{train}} = 500$, whereas $\varepsilon_{\text{tol}}^{\text{RB}} = 5 \times 10^{-2}$. Right: online evaluations of error bounds $\Delta_N(\boldsymbol{\mu})$ (maximum and average over $n_{\text{test}} = 50$ sampled $\boldsymbol{\mu}$ values), Stokes (linear) error bounds $\Delta_{N,s}(\boldsymbol{\mu})$ (average), indicators $\tau_N(\boldsymbol{\mu})$ (maximum) and errors (average and maximum) between FE and RB approximations.

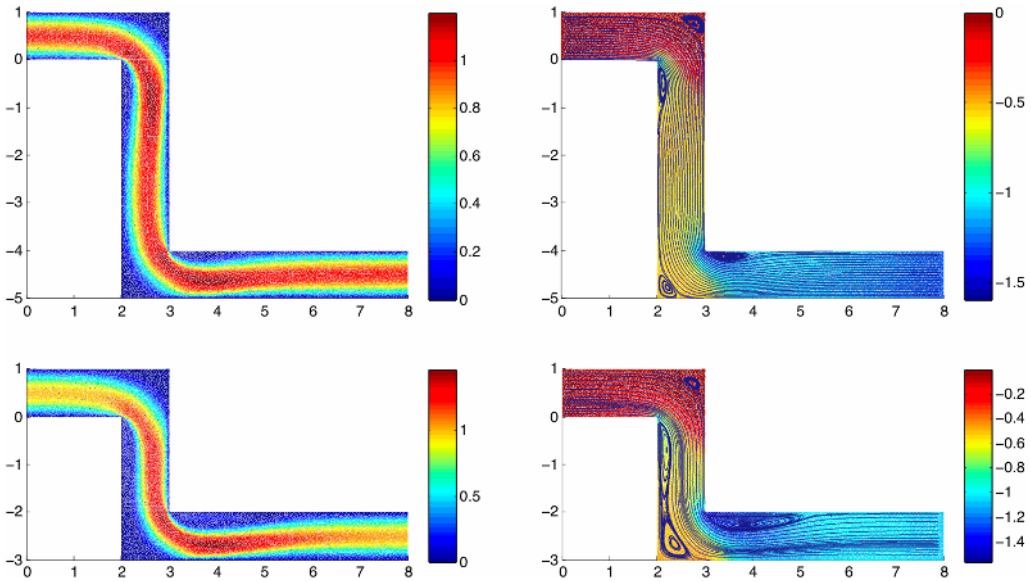

FIGURE 9. Case 2. RB solutions for velocity and pressure for $\boldsymbol{\mu} = (100, 4)$ (top), $\boldsymbol{\mu} = (150, 2)$ (bottom).

Regarding the Online stage, the evaluation of the errors between the FE and the RB approximations (over a train sample Ξ_{test} of size $n_{\text{test}} = 100$, for $N = 1, \ldots, N_{\max}$) and the corresponding error bounds are reported in Figure 8 (right). However, also in this case the effectivity of the error bound is of about 10^2 and the Stokes (linear) error bound $\Delta_{N,s}(\boldsymbol{\mu})$ is very close to $\Delta_N(\boldsymbol{\mu})$ for $N \geq N^*(\boldsymbol{\mu})$.

Finally, we report in Figure 9 some representative solutions. We observe that close to channel corners the flow shows both recirculation regions and detachments which significantly grow when $\mu_1 = Re$ increases.

For the sake of space, we do not report plots of the approximation errors over the spatial domain, which look very similar to the ones shown in Figure 5. As a matter of fact, also in this case pointwise errors over the spatial domain are indeed very small. As we can see in Figure 8 (left), the (norm of) RB approximation errors decreases quite rapidly (from 10^{-2} when $N = 15$, to 10^{-4} when $N = N_{\max} = 30$), uniformly over the parameter space.

9.3. Case 3. Flow around a parametrized NACA airfoil

Finally, we consider the approximation of a steady flow around a family of NACA0012 airfoil profiles (see Fig. 10). In order to change both the orientation and the shape of the airfoil, we parametrize the geometry of the domain $\tilde{\Omega} = \tilde{\Omega}(\boldsymbol{\mu})$ using a nonaffine Free-Form Deformation (FFD) map (see *e.g.* [20]). This is a volume-based parametrization, where deformations are induced by moving some control points, through a set of parameters.

In particular, here a 6×6 lattice of control points is placed around the airfoil and the closest four control points (represented in red) are allowed to move along the x_2-direction, thus giving $p = 4$ parameters (*i.e.* the vertical displacements of the free control points), varying in $\mathcal{D} = [-0.4, 0.4]^4$.

A parabolic flow $\mathbf{g}_D$ is imposed at the inlet $\Gamma_{D_g} = \Gamma_{in}$, such that $|\bar{\mathbf{v}}| = \int_{\Gamma_{in}} \mathbf{g}_D = 20/3$, while a free-stress condition ($\mathbf{g}_N = \mathbf{0}$) is imposed at the outflow $\Gamma_N = \Gamma_{out}$, whereas $\Gamma_{D_0} = \Gamma_B$; the forcing term is $\mathbf{f} = (0, 0)$. Here $Re = 160$ since the characteristic length, *i.e.* the width of the airfoil, is about 0.2.

Concerning the Offline stage, we rely on a $\mathbb{P}_2 - \mathbb{P}_1$ FE approximation also in this case. A further pre-processing is required in this case, in order to recover the affine parametric dependence. To this goal, we employ the EIM procedure (see Sect. 3.2), with a prescribed tolerance $\varepsilon_{tol}^{EIM} = 10^{-4}$; in particular, we prescribe ε_{tol}^{EIM} smaller

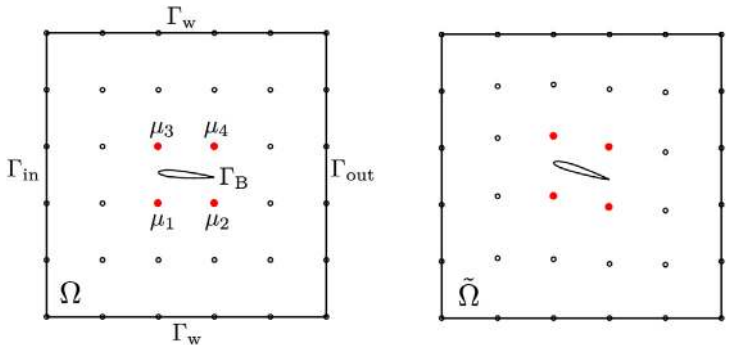

FIGURE 10. Case 3. Parametrized geometry: reference (left) and original (right) configurations.

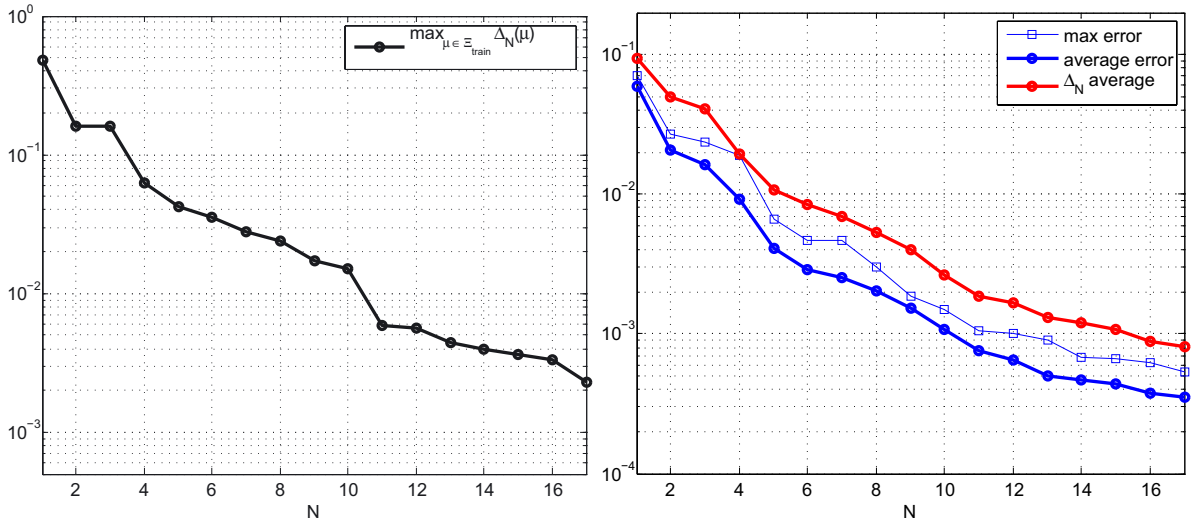

FIGURE 11. Case 3. Left: convergence of the greedy algorithm; here Ξ_{train} is a uniform random sample of size $n_{\text{train}} = 1000$ and RB tolerance is $\varepsilon_{\text{tol}}^{\text{RB}} = 2.5 \times 10^{-3}$. Right: online evaluations of the error bound $\Delta_N(\boldsymbol{\mu})$ (average over $n_{\text{test}} = 100$ sampled $\boldsymbol{\mu}$ values) and the error (average and maximum) between FE and RB approximations.

than the tolerance $\varepsilon_{\text{tol}}^{\text{RB}}$ used as stopping criterion in the greedy procedure. Here the range of variation of the stability factor over the parametric domain, by direct inspection, is rather contained, we opt for a constant lower bound instead of running the SCM procedure. We thus compute a lower bound through a numerical minimization algorithm, based on sequential quadratic programming; in this case, $\beta_{\mathcal{N}}^{LB} = 7.5 \times 10^{-3}$.

Then, we run the greedy algorithm for the construction of the RB spaces; its convergence is reported in Figure 11 (left). In this case, $N_{\max} = 17$ basis functions are selected, with a prescribed tolerance $\varepsilon_{\text{tol}}^{\text{RB}} = 2.5 \times 10^{-3}$.

Regarding the Online stage, the evaluation of the errors between the FE and the RB approximations (over a train sample Ξ_{test} of size $n_{\text{test}} = 100$, for $N = 1, \ldots, N_{\max}$) and the corresponding error bounds are reported in Figure 11 (right). In this case $N^*(\boldsymbol{\mu}) = 1$, so that the error bound $\Delta_N(\boldsymbol{\mu})$ can be employed from the very beginning for both the greedy selection procedure and the online error evaluation. We do not report neither the error indicator $\tau_N(\boldsymbol{\mu})$, nor the Stokes (linear) error bound $\Delta_{N,s}(\boldsymbol{\mu})$, since this latter is very close to $\Delta_N(\boldsymbol{\mu})$.

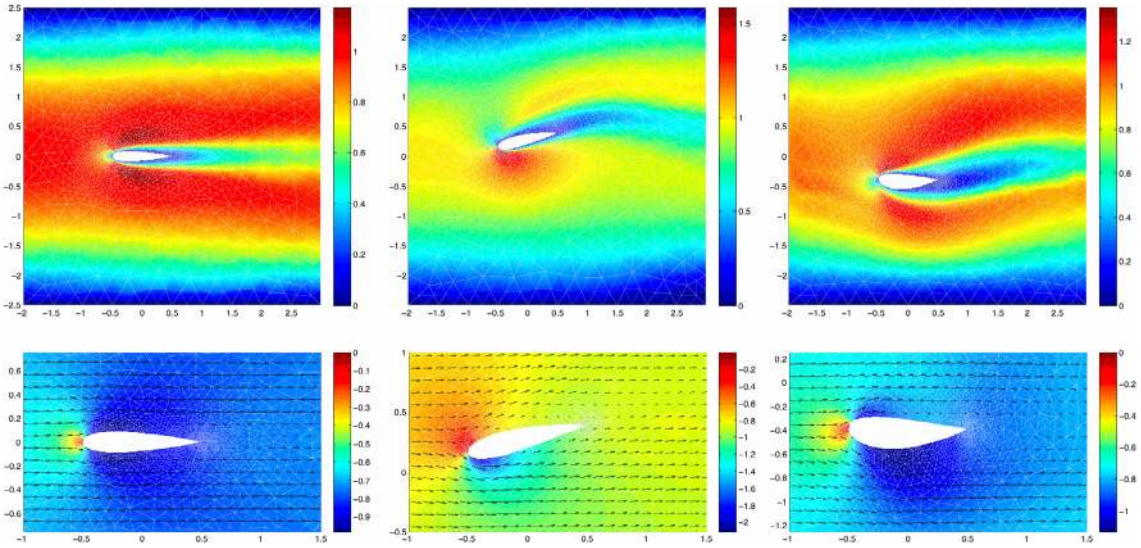

FIGURE 12. Case 3. RB solutions for velocity and pressure for different values of $\boldsymbol{\mu} \in \mathcal{D}$.

Finally, we report in Figure 12 some representative solutions for selected values of the parameters. Also in this case the plots of the approximation errors over the spatial domain look very similar to the ones shown in Figure 5. Moreover, as we can see from Figure 11 (right), the (norm of) RB approximation errors decreases quite rapidly (from 10^{-2} when $N = 4$, to 5×10^{-3} when $N = N_{\max} = 17$), uniformly over the parameter space.

9.4. Summary of results

We can now summarize the computational performances of the RB framework presented in this paper. We report all the details related to numerical simulations in the following Table 1.

The number of affine operator components $Q_a + Q_b + Q_c$ is larger in case 3 compared to other cases, because of the EIM procedure employed to recover the affine parametric dependence in this nonaffine case. We point out that $Q_a + Q_b + Q_c$ can be considered as an index of the parametric complexity of the problem, affecting in particular (i) the storing of RB structures related to nonlinear terms; (ii) the efficient calculation of the dual norms of residuals; (iii) the SCM algorithm for the lower bound of stability factors. In all these cases, larger values of $Q_a + Q_b + Q_c$ might have a great impact on the efficiency of the Offline/Online splitting.

In all the three cases, we remark the very small dimension N of the RB approximation problems with respect to the FE approximation space dimension $\mathcal{N}$, which leads to effective computational savings, mandatory when dealing with numerical simulations in real-time and many-query contexts. The reduction of linear systems dimension ranges between 357 and 699 times; nevertheless, this leads to very small RB approximation errors, of order $10^{-3} \div 10^{-5}$. Computational speedup is of order 10^2, varying from 100 to 564. CPU time for each RB Online evaluation is of order 1 s and is almost constant, also when dealing with the Reynolds number as a parameter. On the other hand, FE solutions require increasing CPU times[6] (and fixed-point iterations) when dealing with larger Reynolds numbers, ranging from about 30 s to 300 s, *e.g.* in case 1. Moreover, with the same tolerance $\varepsilon_{\text{tol}}^{\text{RB}}$ of case 2, we would obtain an even smaller RB space in case 1, of dimension $N_{\max} = 8$, and a larger speedup (about 150) due to an even faster Online evaluation time. On the other hand, the higher speedup of case 2 is also due to the larger FE evaluation time. In this case, a finer computational mesh, and a higher intrinsic difficulty of the problem, play an important role. For both FE and RB solutions of nonlinear problems we use a fixed-point iteration with tolerance $\varepsilon_{\text{tol}}^{NS} = 10^{-5}$.

[6]Computations have been run on a PC with 2×2 GHz Dual Core AMD Opteron (tm) processors 2214 HE and 16 GB of RAM.

TABLE 1. Numerical details for the test cases presented; t_{RB}^{online} is the time of an Online RB computation, while t_{FE}^{online} is the time for a FE computation, once FE linear operators are built.

Approximation data	Case 1	Case 2	Case 3
Number of parameters P	1	2	4
Affine op. components $Q_a + Q_b + Q_c$	9	18	77
Affine rhs components $Q_F + Q_G$	9	13	67
FE space dim. $\mathcal{N}$	23 077	31 093	32 538
RB space dim. $N_{\max}$	12	31	17
FE evaluation $t_{\text{FE}}^{\text{online}}$ (s)	137.47	2070.25	460.28
RB evaluation $t_{\text{RB}}^{\text{online}}$ (s)	1.3707	3.667	1.2201
Computational speedup	100	564	377
FE stability factor evaluation $t_{\text{stab}}^{\text{offline}}$ (s)	1436	51 644	688
RB space construction $t_{\text{space}}^{\text{offline}}$ (s)	5303	73 028	12 984
Break-even point $\mathcal{Q}_{BE}$	49	60	29

Finally, we take into account also the time spent for the Offline construction and storage; this allows to determine the break-even point, given by $\mathcal{Q}_{BE} = (t_{\text{stab}}^{\text{offline}} + t_{\text{space}}^{\text{offline}})/t_{FE}^{\text{online}}$. In particular, we obtain a break-even point smaller than 10^2 in all the three cases.

We point out that the SCM algorithm require very large CPU times, ranging from 1436 s (case 1) to 51644 s (case 2); this corresponds, respectively, to 21% and 41% of the whole Offline stage. Instead, evaluating the (constant) lower bound through a numerical optimization procedure takes just the 5% of the whole Offline CPU time in case 3. An additional computational cost is entailed, in this latter case, by the EIM procedure used to recover the affine parameter dependence. If the same SCM was used to generate a variable lower bound $\beta_{\mathcal{N}}^{LB}(\boldsymbol{\mu})$ instead of using a constant, the required CPU time would have been considerably larger (at least as large as in case 2). This is due to the number of parameter components and to the (considerably) larger number of affine components, and would lead to a break-even point of about $\mathcal{Q}_{BE} \approx 150$. See also [18] for further comparisons between the SCM algorithm and some heuristic procedures to obtain reliable surrogates of stability factors.

10. Remarks and conclusions

In this paper we have presented a self-contained mathematical framework for the set up of the reduced basis approximation and *a posteriori* estimation in the case of steady incompressible parametrized Navier–Stokes equations. We have considered a mixed formulation for velocity and pressure fields, with (both affine and non-affine) physical and geometrical parametrizations; we have taken advantage of a recent extension [18] of the natural norm SCM algorithm to nonlinear operators; we have developed a suitable Offline/Online computational splitting. In this way, we have managed to fully decouple the estimation of stability factors and the construction of a reduced space through a greedy selection of velocity-pressure snapshots. In particular, the greedy algorithm enables to build reduced spaces of limited dimension also in the case of parametrized steady NS problems, thus yielding a remarkable computational speedup with respect to full-order FE approximations. Several numerical tests have proved the computational efficiency and the reliability of the proposed methodology. Other applications have already been presented *e.g.* in [15, 19]. Further developments will be devoted to the application of this framework to optimal control problems for fluid flows.

Acknowledgements. I thank Prof. A. Quarteroni (Politecnico di Milano and EPFL) for his valuable comments and many contributions and Federico Negri (EPFL) for his great help in performing some of the numerical simulations presented in this work. I am grateful to Dr. G. Rozza (SISSA) and Dr. T. Lassila (EPFL) for many discussions on the subject, and to Prof. A.T. Patera (MIT) for his feedbacks and suggestions. This work has been supported by the Swiss National Science Foundation (Projects 122136 and 135444) and by the SHARM 2012-2014 SISSA post-doctoral research grant on the project "Reduced Basis Methods for shape optimization in computational fluid dynamics".

Appendix A. Computational details and proofs

In this Appendix we report the proofs of the results stated in Sections 6 and 8, as well as some computational details related to the Offline/Online strategy to deal with the efficient construction of RB structures.

A.1. Offline-Online computational strategy

Thanks to the affine parametric expansions of Section 3.2, we can write the matrices occurring in the FE formulation by decoupling the $\boldsymbol{\mu}$-dependent and $\boldsymbol{\mu}$-independent parts: for the linear terms we have

$$\mathbb{A}_{\mathcal{N}}(\boldsymbol{\mu}) = \sum_{q=1}^{Q_a} \Theta_a^q(\boldsymbol{\mu}) \mathbb{A}_{\mathcal{N}}^q, \qquad \mathbb{B}_{\mathcal{N}}(\boldsymbol{\mu}) = \sum_{q=1}^{Q_b} \Theta_b^q(\boldsymbol{\mu}) \mathbb{B}_{\mathcal{N}}^q, \tag{A.1}$$

being $(\mathbb{A}_{\mathcal{N}}^q)_{ij} = a^q(\boldsymbol{\phi}_j^{\mathbf{v}}, \boldsymbol{\phi}_i^{\mathbf{v}})$, $1 \le q \le Q_a$ and $(\mathbb{B}_{\mathcal{N}}^q)_{ki} = b^q(\phi_k^p, \boldsymbol{\phi}_i^{\mathbf{v}})$, $1 \le q \le Q_b$; for the nonlinear terms, with $1 \le q \le Q_c$, we have instead

$$\mathbb{C}_{\mathcal{N}}(\underline{\mathbf{w}}_{\mathcal{N}}; \boldsymbol{\mu}) = \sum_{q=1}^{Q_c} \Theta_c^q(\boldsymbol{\mu}) \mathbb{C}_{\mathcal{N}}^q(\underline{\mathbf{w}}_{\mathcal{N}}), \quad (\mathbb{C}_{\mathcal{N}}^q(\underline{\mathbf{w}}_{\mathcal{N}}))_{ij} = c^q \left(\sum_{k=1}^{\mathcal{N}_V} w_k^{\mathcal{N}} \boldsymbol{\phi}_k^{\mathbf{v}}, \boldsymbol{\phi}_j^{\mathbf{v}}, \boldsymbol{\phi}_i^{\mathbf{v}} \right); \tag{A.2}$$

a similar expansion can be obtained for $\mathbb{D}_{\mathcal{N}}(\boldsymbol{\mu})$ and the right-hand sides. Thanks to the affine decomposition in (A.1)–(A.2), we can rewrite the matrices in (5.9) as

$$\begin{aligned}
\mathbb{A}_N(\boldsymbol{\mu}) &= \sum_{q=1}^{Q_a} \Theta_q^a(\boldsymbol{\mu}) \mathbb{A}_N^q, & \mathbb{A}_N^q &= \mathbb{V}_N^T \, \mathbb{A}_{\mathcal{N}}^q \, \mathbb{V}_N, \\
\mathbb{B}_N(\boldsymbol{\mu}) &= \sum_{q=1}^{Q_b} \Theta_q^b(\boldsymbol{\mu}) \mathbb{B}_N^q, & \mathbb{B}_N^q &= \mathbb{Q}_N^T \, \mathbb{B}_{\mathcal{N}}^q \, \mathbb{V}_N, \\
\mathbb{C}_N\left(\underline{\boldsymbol{\zeta}}_s^{\mathbf{v}}; \boldsymbol{\mu}\right) &= \sum_{q=1}^{Q_c} \Theta_q^c(\boldsymbol{\mu}) \mathbb{C}_N^q\left(\underline{\boldsymbol{\zeta}}_s^{\mathbf{v}}\right), & \mathbb{C}_N^q\left(\underline{\boldsymbol{\zeta}}_s^{\mathbf{v}}\right) &= \mathbb{V}_N^T \, \mathbb{C}_{\mathcal{N}}^q\left(\underline{\boldsymbol{\zeta}}_s^{\mathbf{v}}\right) \, \mathbb{V}_N.
\end{aligned} \tag{A.3}$$

In the same way, we can express the RB structures appearing in (5.10).

Thus, in the *Offline stage* we first compute and store the basis functions $\{\boldsymbol{\zeta}_n^{\mathbf{v}}\}_{n=1}^{2N}$, $\{\zeta_l^p\}_{l=1}^{N}$, and form the RB structures. In the *Online stage*, for each new value of $\boldsymbol{\mu}$ we use the precomputed RB structures to assemble the (full) $3N \times 3N$ system (5.7). Hence, Online costs are dependent on $Q_\bullet$ and N, but independent of $\mathcal{N}_X + \mathcal{N}_Q$: since $3N \ll \mathcal{N}_X + \mathcal{N}_Q$, we obtain a significant speedup in the Online stage compared to the pure FE approach. Moreover, we may choose $\mathcal{N}$ very large in order to eliminate the error between the exact solution and the FE approximations without affecting the RB Online efficiency – for instance, when dealing with moderate Reynolds numbers. In fact, the bigger the underlying FE system and thus $\mathcal{N}$ is chosen, the bigger the speedup by the use of the RB method in the Online stage will be. However, we should keep in mind that the Offline stage is still $\mathcal{N}$-dependent.

A.2. Proof of Lemma 8.1

Let us recall that

$$\max_{\substack{v \in V^{\mathcal{N}} \\ (v,v)_V = 1}} \left(u_*^2, v^2\right) = \frac{\|u_*^2\|_2^2}{(u_*, u_*)_V^2}$$

by Cauchy–Schwarz inequality, since $(u_*^2, v^2)_2 \le \|u_*^2\|_2 \|v^2\|_2$ and the maximum is reached for an element $v = \alpha u_*$ where $\alpha = 1/(u_*, u_*)_V$. Thanks to (8.4) and (8.2), we find

$$\lambda_{\max}\left(\sigma(u_*)\right) = \max_{v \in V^{\mathcal{N}}} \frac{\int_\Omega u_*^2 v^2}{\|u_*\|_4^2 (v,v)_V} = \max_{\substack{v \in V^{\mathcal{N}} \\ (v,v)_V = 1}} \frac{\int_\Omega u_*^2 v^2}{\|u_*\|_4^2} = \frac{\int_\Omega u_*^4}{\|u_*\|_4^2 \, (u_*, u_*)_V^2} = \frac{\|u_*\|_4^2}{(u_*, u_*)_V^2} = \rho^2, \tag{A.4}$$

since $(u_*, u_*)_V = 1$. Since $u_{\max}(z)$ is the maximizer of (8.4), *i.e.* it is such that

$$u_{\max}(z) = \arg\max_{v \in V^{\mathcal{N}}} \left(\frac{1}{(v,v)_V} \int_\Omega z v^2 \right),$$

from (A.4) and $(u_*, u_*)_V = 1$ we obtain $u_{\max}(\sigma(u_*)) = u_*/((u_*, u_*)_V) = u_*$.

A.3. Proof of Lemma 8.2

It is clear that $u_{\max}(z_2) - u_{\max}(z_1) = \mathcal{O}(\|z_2 - z_1\|_2)$ and $\lambda_{\max}(z_2 - z_1) = \mathcal{O}(\|z_2 - z_1\|_2)$. Then, the last term of (8.5) is at least $\mathcal{O}(\|z_2 - z_1\|_V)$. Then, by definition of the eigenproblem (8.3), we have:

$$\int_\Omega z_2 u_{\max}(z_2)(\partial u) = \lambda_{\max}(z_2)(u_{\max}(z_2), \partial u)_V, \tag{A.5}$$

$$\int_\Omega z_1 u_{\max}(z_1)(\partial u) = \lambda_{\max}(z_1)(u_{\max}(z_1), \partial u)_V. \tag{A.6}$$

To simplify these expressions, we exploit the two relationships (valid for any A, B and any inner product)

$$\begin{aligned}(A - B, A) &= \frac{1}{2}(A, A) - \frac{1}{2}(B, B) + \frac{1}{2}(A - B, A - B),\\ (B - A, A) &= \frac{1}{2}(A, A) - \frac{1}{2}(B, B) - \frac{1}{2}(A - B, A - B),\end{aligned} \tag{A.7}$$

by applying the former to the right-hand side of (A.5) with $A = u_{\max}(z_2)$, $B = u_{\max}(z_1)$ and the latter to the right-hand side (A.6) with $A = u_{\max}(z_1)$, $B = u_{\max}(z_2)$, respectively. Since $\|u_{\max}(z_i)\|_V = 1$ for $i = 1, 2$, we end up with

$$\begin{aligned}\int_\Omega z_2 u_{\max}(z_2)(u_{\max}(z_2) - u_{\max}(z_1)) &= \frac{1}{2}\lambda_{\max}(z_2)\|u_{\max}(z_2) - u_{\max}(z_1)\|_V^2,\\ \int_\Omega z_1 u_{\max}(z_2)((u_{\max}(z_2) - u_{\max}(z_1)) &= -\frac{1}{2}\lambda_{\max}(z_1)\|u_{\max}(z_1) - u_{\max}(z_2)\|_V^2,\end{aligned}$$

which proves the thesis.

In the same way, (8.7) is positive thanks to (A.7) – with $A = \sigma(u_{\max}(z^{(k-1)}))$ and $B = \sigma(u_{\max}(z^{(k-2)}))$ – and because $\|\sigma(u_{\max}(z^{(k-1)}))\|_2 = \|\sigma(u_{\max}(z^{(k-2)}))\|_2 = 1$.

References

[1] M. Barrault, Y. Maday, N.C. Nguyen and A.T. Patera, An "empirical interpolation" method: application to efficient reduced-basis discretization of partial differential equations. *C. R. Math. Acad. Sci. Paris* **339** (2004) 667–672.

[2] G. Biswas, M. Breuer and F. Durst, Backward-facing step flows for various expansion ratios at low and moderate Reynolds numbers. *J. Fluids Eng.* **126** (2004) 362–374.

[3] F. Brezzi, On the existence, uniqueness, and approximation of saddle point problems arising from Lagrangian multipliers. *RAIRO. Anal. Numér.* **2** (1974) 129–151.

[4] F. Brezzi, J. Rappaz and P.A. Raviart, Finite dimensional approximation of nonlinear problems. Part I: Branches of nonsingular solutions. *Numer. Math.* **36** (1980) 1–25.

[5] G. Caloz and J. Rappaz, Numerical analysis for nonlinear and bifurcation problems. In vol. 5, Techniques of Scientific Computing (Part 2). *Handbook of Numerical Analysis*, edited by P.G. Ciarlet and J.L. Lions. Elsevier Science B.V. (1997) 487–637.

[6] C. Canuto, T. Tonn and K. Urban, *A posteriori* error analysis of the reduced basis method for non-affine parameterized nonlinear pdes. *SIAM J. Numer. Anal.* **47** (2009) 2001–2022.

[7] S. Deparis, Reduced basis error bound computation of parameter-dependent Navier–Stokes equations by the natural norm approach. *SIAM J. Numer. Anal.* **46** (2008) 2039–2067.

[8] S. Deparis and G. Rozza, Reduced basis method for multi-parameter-dependent steady Navier-Stokes equations: Applications to natural convection in a cavity. *J. Comput. Phys.* **228** (2009) 4359–437.

[9] H.C. Elman, D.J. Silvester and A.J. Wathen, Finite Elements and Fast Iterative Solvers with Applications in Incompressible Fluid Dynamics. *Series in Numer. Math. Sci. Comput.* Oxford Science Publications, Clarendon Press, Oxford (2005).

[10] A.-L. Gerner and K. Veroy, Reduced basis a posteriori error bounds for the Stokes equations in parametrized domains: a penalty approach. *Math. Models Methods Appl. Sci.* **21** (2010) 2103–2134.

[11] P.M. Gresho and R.L. Sani, *Incompressible Flow and the Finite Element Method: Advection-Diffusion and Isothermal Laminar Flow.* John Wiley & Sons (1998).

[12] H. Herrero, Y. Maday and F. Pla, RB (reduced basis) for RB (Rayleigh-Bénard). *Comput. Methods Appl. Mech. Engrg.* **261–262** (2013) 132–141.

[13] D.B.P. Huynh, D.J. Knezevic, Y. Chen, J.S. Hesthaven and A.T. Patera, A natural-norm successive constraint method for inf-sup lower bounds. *Comput. Methods Appl. Mech. Engrg.* **199** (2010) 1963–1975.

[14] K. Ito and S.S. Ravindran, A reduced order method for simulation and control of fluid flows. *J. Comput. Phys.* **143** (1998) 403–425.

[15] T. Lassila, A. Manzoni, A. Quarteroni and G. Rozza, Boundary control and shape optimization for the robust design of bypass anastomoses under uncertainty. *ESAIM: M2AN* **47** (2013) 1107–1131.

[16] T. Lassila, A. Manzoni, A. Quarteroni and G. Rozza, Model order reduction in fluid dynamics: challenges and perspectives. In vol. 9, *Reduced Order Methods for Modeling and Computational Reduction*. Edited by A. Quarteroni and G. Rozza. Springer MS&A Series (2014) 235–274.

[17] A. Manzoni, *Reduced models for optimal control, shape optimization and inverse problems in haemodynamics*. Ph.D. thesis, École Polytechnique Fédérale de Lausanne (2012).

[18] A. Manzoni and F. Negri, Rigorous and heuristic strategies for the approximation of stability factors in nonlinear parametrized PDEs. Technical report MATHICSE 8.2014: `http://mathicse.epfl.ch/`, submitted (2014).

[19] A. Manzoni, A. Quarteroni and G. Rozza, Model reduction techniques for fast blood flow simulation in parametrized geometries. *Int. J. Numer. Methods Biomed. Engrg.* **28** (2012) 604–625.

[20] A. Manzoni, A. Quarteroni and G. Rozza, Shape optimization of cardiovascular geometries by reduced basis methods and free-form deformation techniques. *Int. J. Numer. Methods Fluids* **70** (2012) 646–670.

[21] N.C. Nguyen, K. Veroy and A.T. Patera, Certified real-time solution of parametrized partial differential equations. *Handbook of Materials Modeling*. Edited by S. Yip. Springer, The Netherlands (2005) 1523–1558.

[22] J.S. Peterson, The reduced basis method for incompressible viscous flow calculations. *SIAM J. Sci. Statis. Comput.* **10** (1989) 777–786.

[23] A. Quarteroni and G. Rozza, Numerical solution of parametrized Navier-Stokes equations by reduced basis methods. *Numer. Methods Partial Differ. Equ.* **23** (2007) 923–948.

[24] A. Quarteroni, G. Rozza and A. Manzoni, Certified reduced basis approximation for parametrized partial differential equations in industrial applications. *J. Math. Ind.* **1** (2011).

[25] A. Quarteroni and A. Valli, *Numerical Approximation of Partial Differential Equations* 1st edition. Springer-Verlag, Berlin-Heidelberg (1994).

[26] G. Rozza, D.B.P. Huynh and A. Manzoni, Reduced basis approximation and a posteriori error estimation for Stokes flows in parametrized geometries: roles of the inf-sup stability constants. *Numer. Math.* **125** (2013) 115–152.

[27] G. Rozza, D.B.P. Huynh and A.T. Patera, Reduced basis approximation and a posteriori error estimation for affinely parametrized elliptic coercive partial differential equations. *Arch. Comput. Methods Engrg.* **15** (2008) 229–275.

[28] G. Rozza and K. Veroy, On the stability of reduced basis methods for Stokes equations in parametrized domains. *Comput. Methods Appl. Mech. Engrg.* **196** (2007) 1244–1260.

[29] S. Sen, K. Veroy, D.B.P. Huynh, S. Deparis, N.C. Nguyen and A.T. Patera, "Natural norm" a posteriori error estimators for reduced basis approximations. *J. Comput. Phys.* **217** (2006) 37–62.

[30] R. Temam, *Navier-Stokes Equations*. AMS Chelsea, Providence, Rhode Island (2001).

[31] K. Veroy and A.T. Patera, Certified real-time solution of the parametrized steady incompressible Navier-Stokes equations: rigorous reduced-basis a posteriori error bounds. *Int. J. Numer. Methods Fluids* **47** (2005) 773–788.

[32] M. Yano and A.T. Patera, A space-time variational approach to hydrodynamic stability theory. *Proc. R. Soc. A* **469** (2013) 0036.